JINA–CEE

Separator Ion Optics School

NSCL, Michigan State University

Series of Four Lectures plus COSY Tutorials
September 10-14, 2018

Georg P. Berg
University of Notre Dame
JINA Center for the Evolution of the Elements

The Lecture Series

An Introduction to Ion-Optics

1st Lecture: 9/10/18: Formalism and ion-optical elements

2nd Lecture: 9/12/18: Ion-optical systems and spectrometers

3rd Lecture: 9/12/18: Recoil separators for nuclear astrophysics, St. GEORGE

4rd Lecture: 9/13/18: The recoil separator SECAR for FRIB

Tutorials in the afternoon: 9/10/18 – 9/14/18: COSY Infinity

Review 2nd Lecture

Ion-optical systems, spectrometers

High resolution spectrometers

Full dispersion matching

Diagnostics and field measurements.

Observing faint radiation near the sun:

An analogy for observing nuclear particles close to the beam

Solar Eclipse
Coronagraph

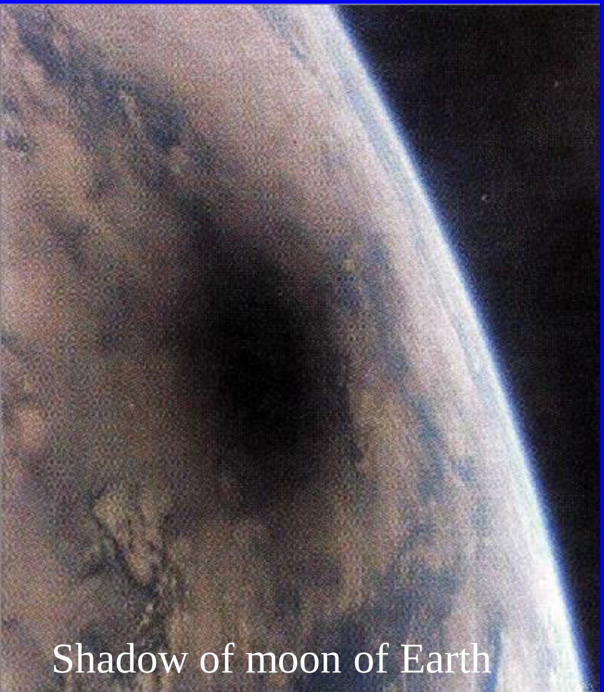

Shadow of moon of Earth

Solar Eclipse 1999

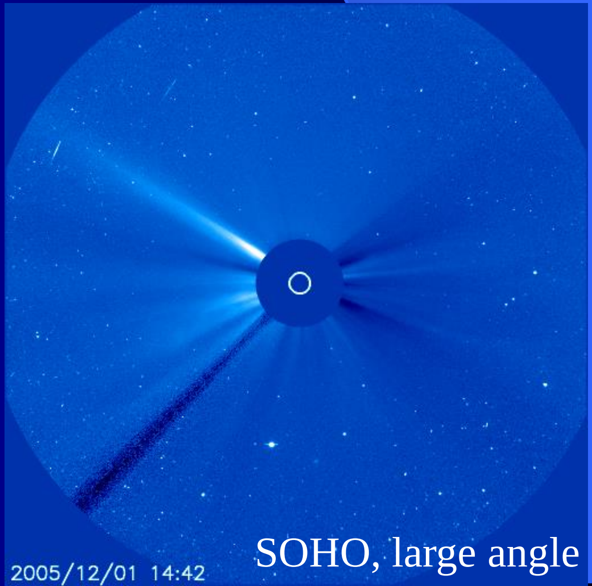

SOHO, large angle

The Chromosphere of the Sun in Hα

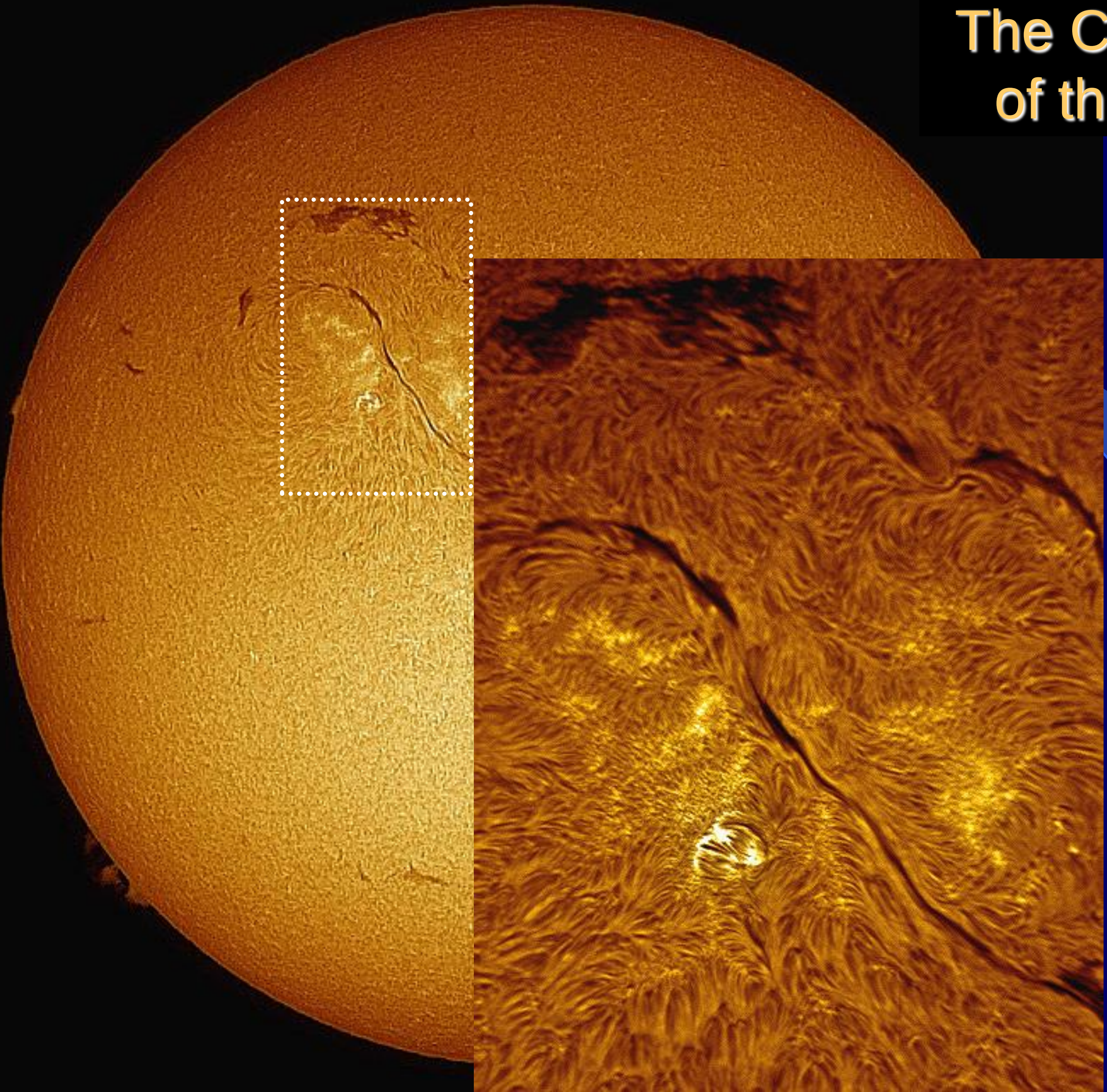

Hα line, λ = 656.28nm

Δλ = 0.07nm
Narrow Band Filter

Magnetic (Bρ) Separation of Beam & Reaction Products in Spectrometer Experiments near 0^o

K600, Grand Raiden Spectrometers:

(^{3}He,t), (p,t), (α,α'), (p,p'), (α,^{8}He)

Special Faraday cups to stop beam inside spectrometer or near focal plane

K600 Spectrometer (IUCF)

The K600 is shown in 0^o Transmission mode for inelastic scattering at 0^o

High Dispersion Plane
B(D1) > B(D2)

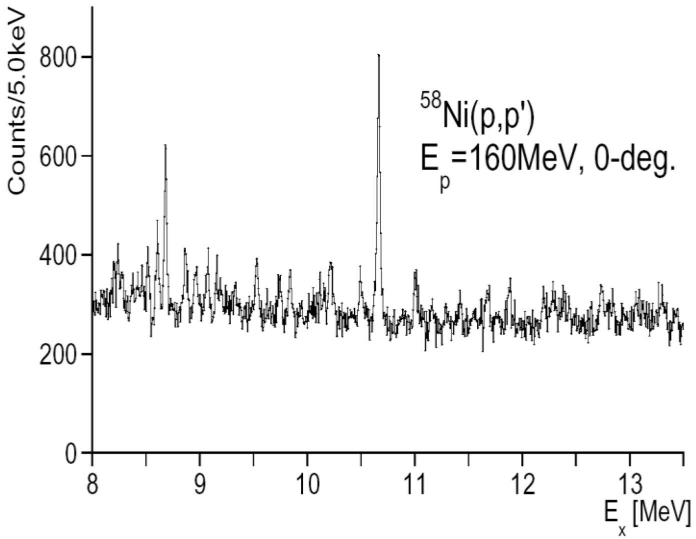

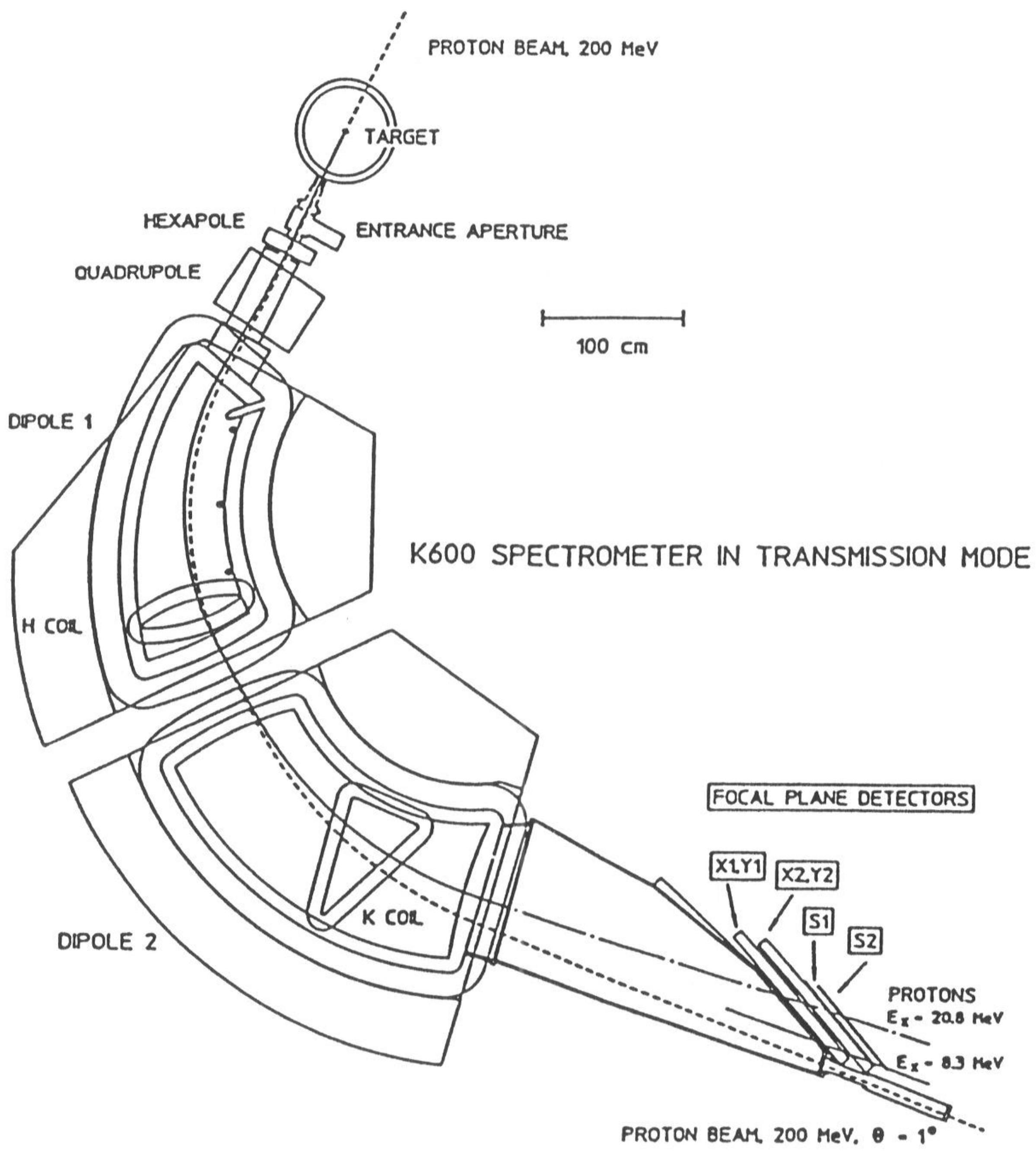

Grand Raiden High Resolution Spectrometer

Grand Raiden is shown in
0^o Transmission mode
for reactions at 0^o

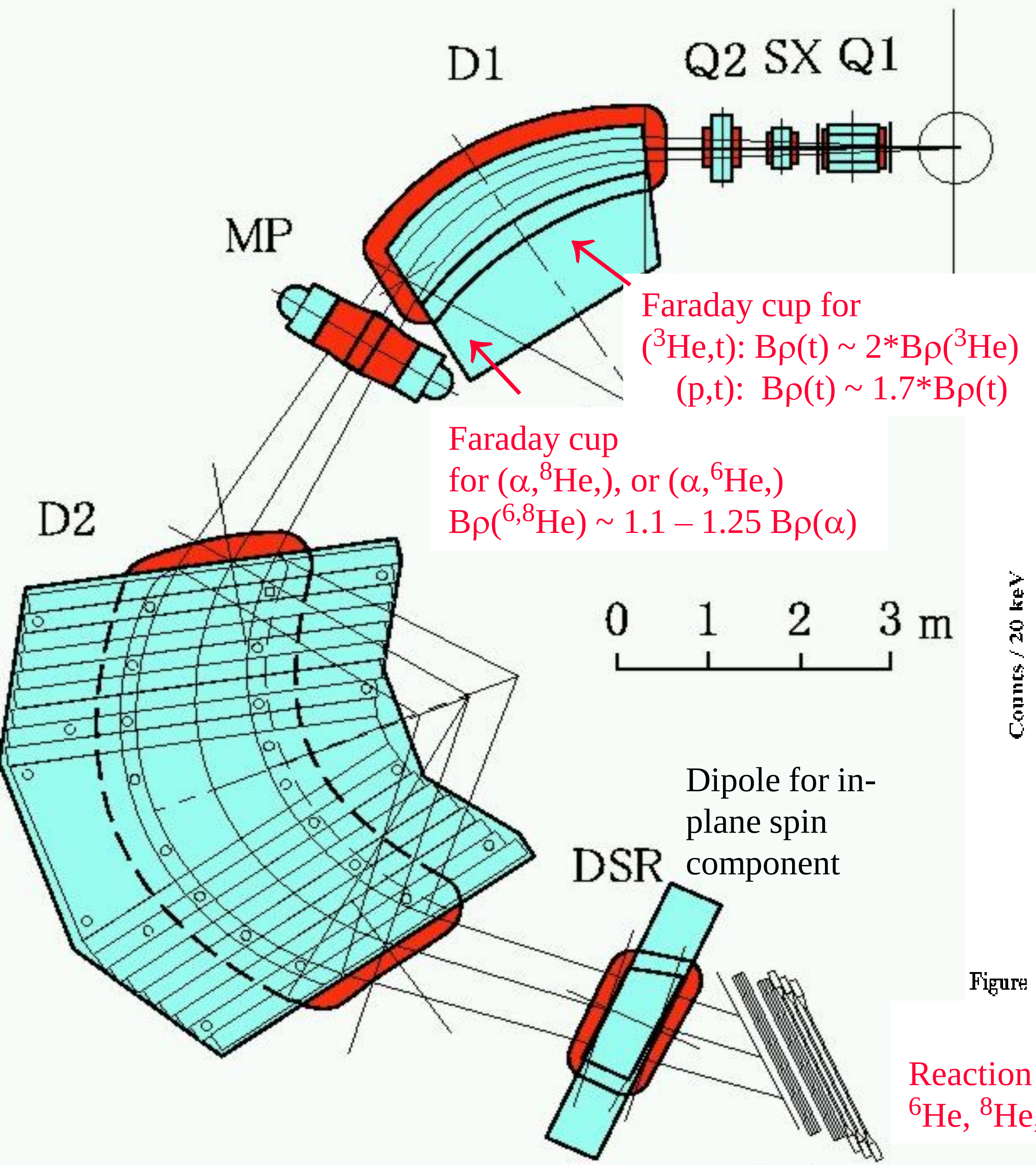

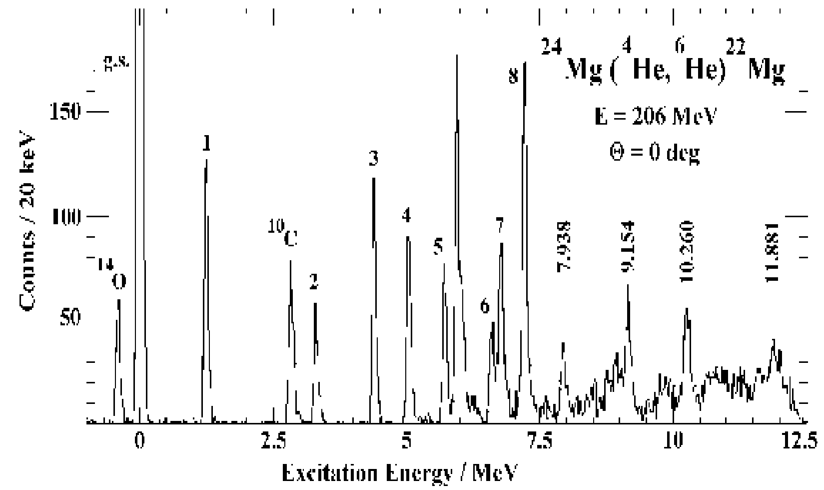

Figure 1. Measured ^{22}Mg spectrum with angle cut 0 - 1.5° and a resolution of 75 keV.

Reaction Products
^{6}He, ^{8}He, t

Nucleosynthesis in the Cosmos

Superheavy Elements in Laboratories

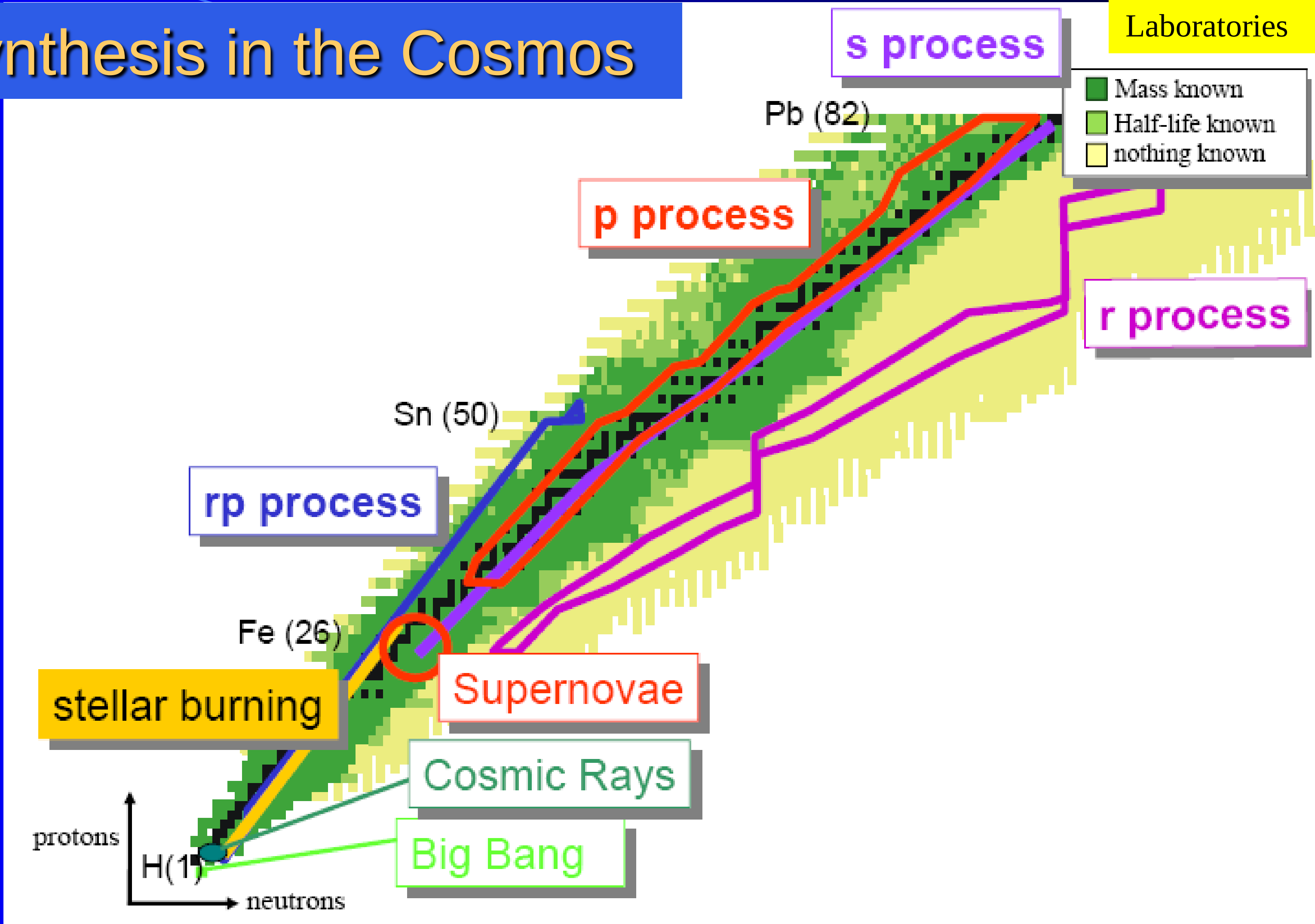

Many different reactions are involved in the nuclei synthesis

With recoil separators, we study the important (p,γ) and (α,γ) radiative capture reactions that take place e.g. in the rp process.

Example: $^{22}Ne(\alpha,n)^{25}Mg$, $^{22}Ne(\alpha,\gamma)^{26}Mg$

The potential existence of low energy resonances causes considerable uncertainty in reaction rate
Stable Beams: St. GEORGE
RI Beams: SECAR

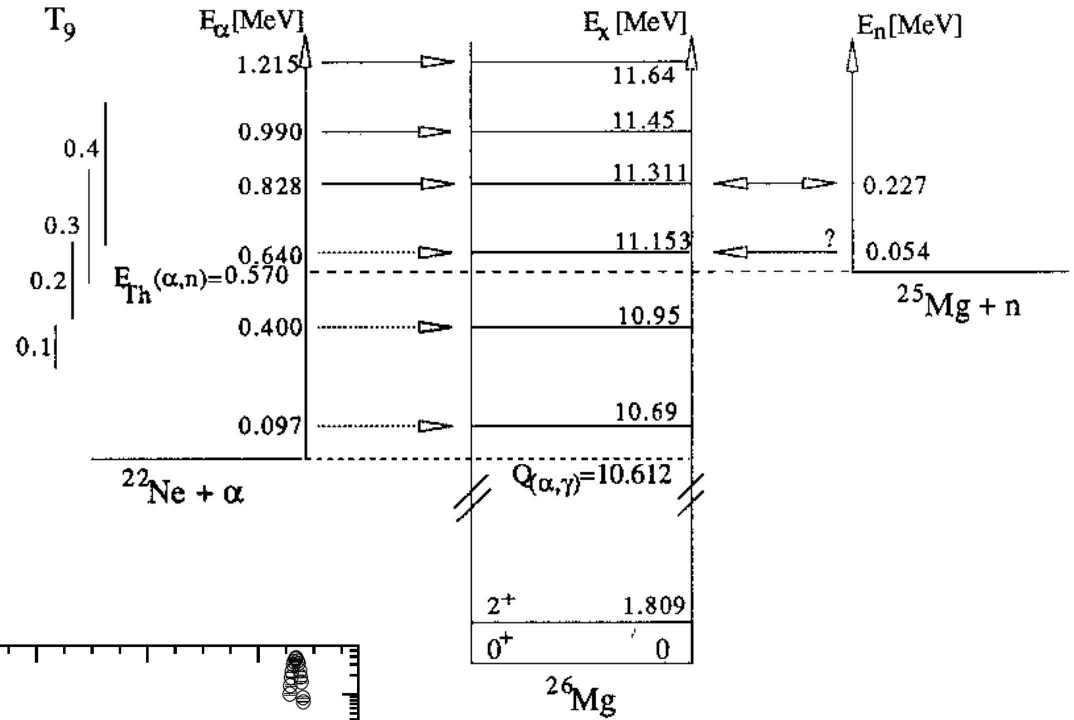

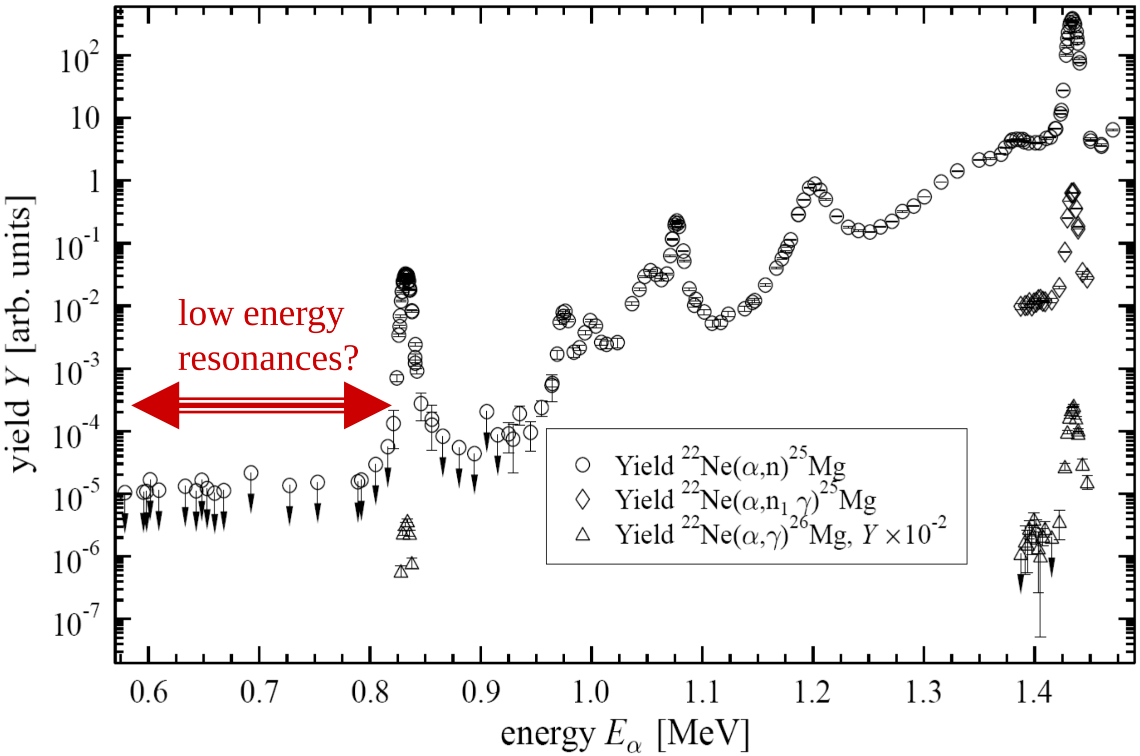

Low energy resonances
Cannot be measure due to low cross sections that do not rise above background from:

1) Cosmic rays
2) Surrounding radio-active materials
3) Beam-related background

Solutions:

1) Go underground (Salt mine!)
2) Inverse kinematics (recoil separator)

Rigidity and Acceptance Parameters Determined by Reaction Kinematics and Target Effects

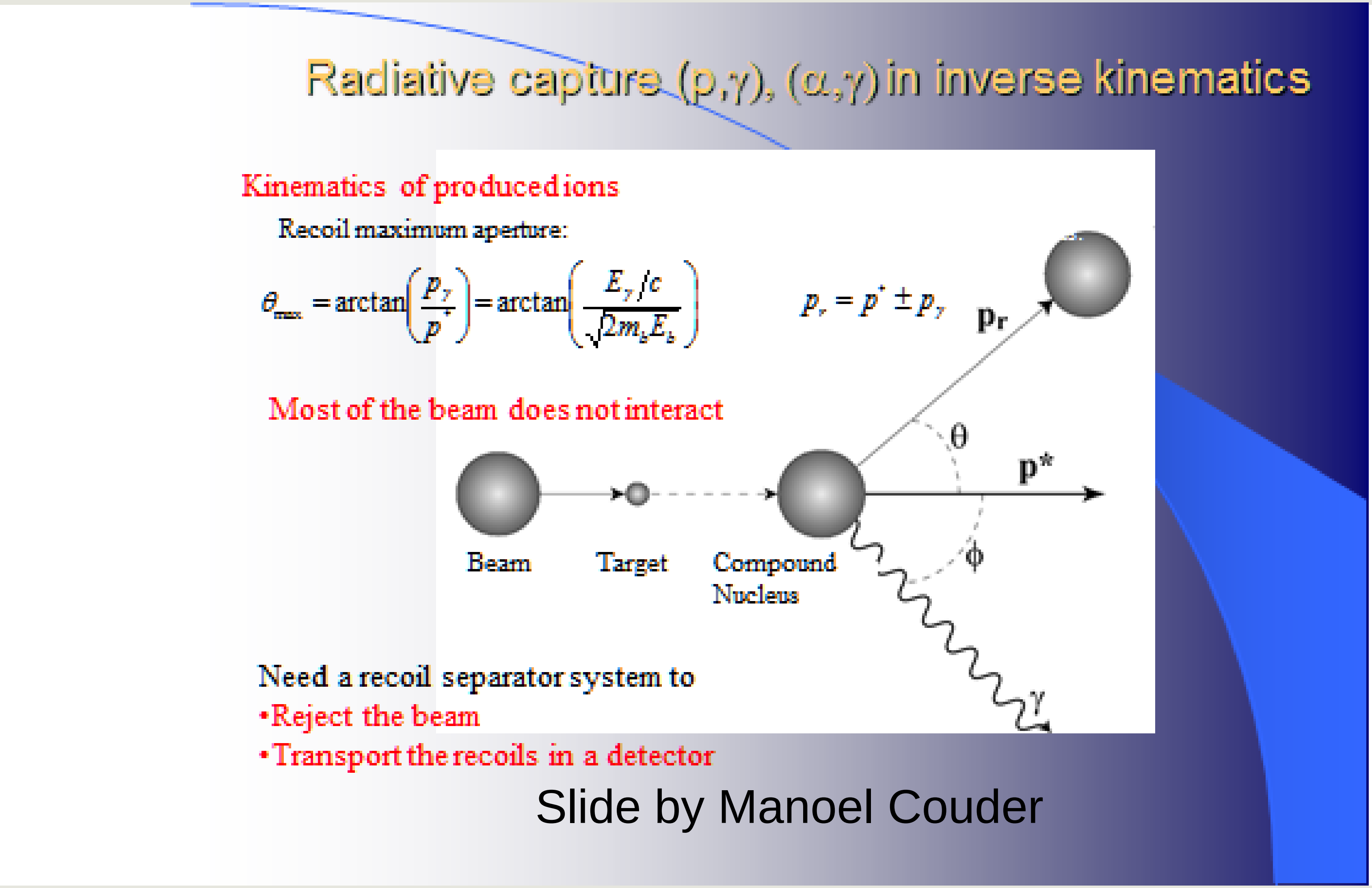

Slide by Manoel Couder

St. George

Reactions and Design Parameters

Table 1
Design parameters of the St. George magnetic recoil separator.

Maximum rigidity $B\rho$	0.45 Tm
Minimum rigidity $B\rho$	0.1 Tm
Angle acceptance, vert., horiz	±40 mrad
Energy acceptance	± 7.5 %
Mass separation $m/\Delta m$	≈ 100
Bending radius	75 cm

Beam and recoils have same momenta, need E field for separation.

Table 2
Sample of reactions of astrophysical interest

		Inverse (α,γ) reaction								
Beam	Recoil	Beam E_{lab} MeV	E_{cm} MeV	Recoil E_{lab} MeV	Recoil Q[9]	Recoil Abund. %	Half Angle mrad	E Range ±%	Mom. p MeV/c	$B\rho$ T/m
^{16}O	^{20}Ne	5.80	1.16	4.640	5	42	14.2	2.8	415.7	0.277
		12.5	2.50	10.02	6	40	11.8	2.4	610.9	0.340
^{18}O	^{22}Ne	1.94	0.35	1.591	3	38	39.2	7.8	177.1	0.284
		3.30	0.60	2.700	4	42	30.9	6.2	332.6	0.277
^{34}S	^{38}Ar	10.0	1.05	8.950	8	32	10.4	2.1	795.7	0.332
		38.0	4.00	34.00	12	32	7.20	1.4	1551	0.431
^{36}Ar	^{40}Ca	12.5	1.25	11.25	9	31	9.10	1.8	915.3	0.339
		40.0	4.00	36.00	13	30	6.70	1.3	1638	0.420

Achromatic magnet separator

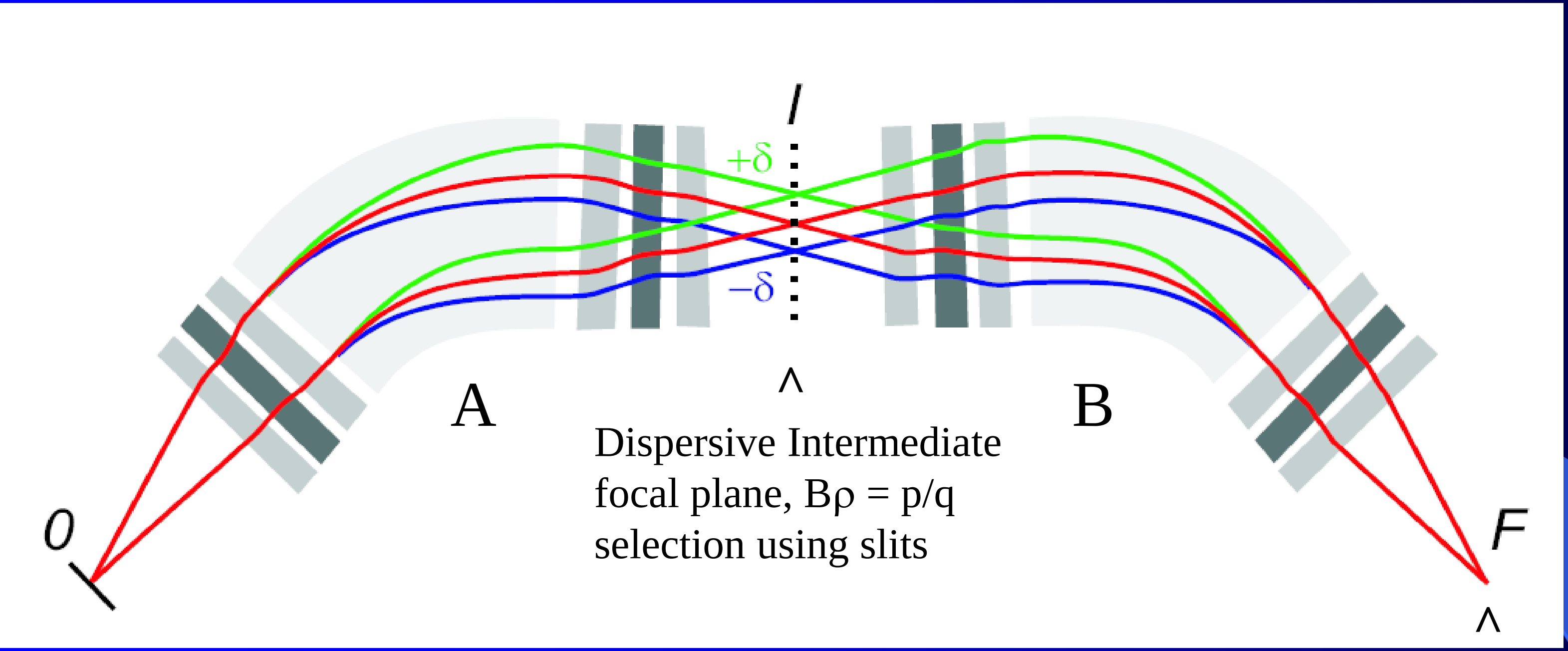

Figure from Experimental Techniques at NSCL, MSU, Th. Baumann, 8/2/2002

Achromatic Final focal plane, small beam spot e.g. for detector system

Assume foci at I & F, i.e. $A_{12} = B_{12} = 0$. Derive the first order achromatic condition of the system 0 → F and compare with the dispersion matching condition.

Solution of Exercise

First order TRANSPORT Matrix $R_{\mu\nu}$

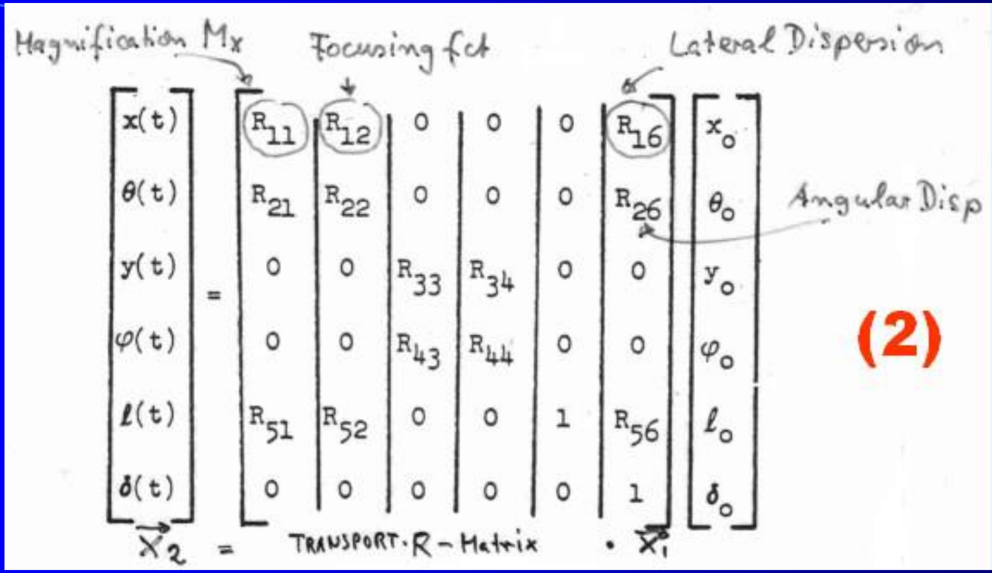

(2)

$$x_I = A_{11}\, x_0 + A_{12}\, \theta_0 + A_{16}\, \delta_0 \qquad |\ A_{12} = 0$$

$$= A_{11}\, x_0 + A_{16}\, \delta_0 \qquad \textbf{(25)}$$

$$x_F = B_{11}\, x_I + B_{12}\, \theta_I + B_{16}\, \delta_0 \qquad |\ B_{12} = 0$$

$$= B_{11}\, x_I + B_{16}\, \delta_0 \qquad |\ \text{substitute } x_I \text{ using } \textbf{(25)}$$

$$= B_{11}\, (A_{11}\, x_0 + A_{16}\, \delta_0) + B_{16}\, \delta_0$$

$$= B_{11}\, A_{11}\, x_0 + (B_{11}\, A_{16} + B_{16}\,)\, \delta_0$$

Condition for achromaticity: $A_{16} = - B_{16} / B_{11}$

Note: This is the Dispersion Matching condition for C = T = 1

Achromatic magnet separator

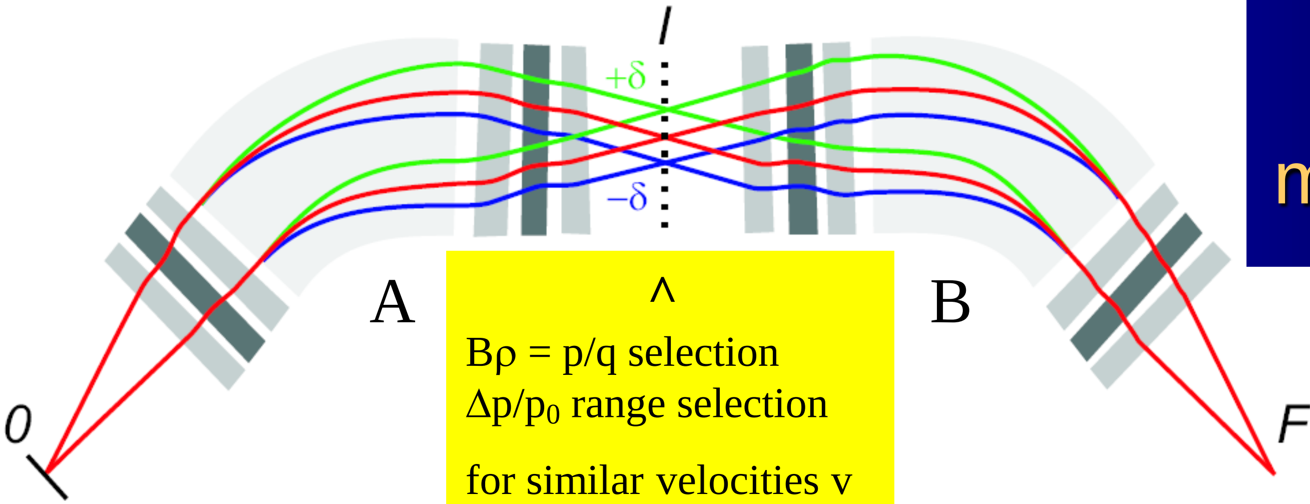

^

$B\rho = p/q$ selection
$\Delta p/p_0$ range selection

for similar velocities v
m/q selection,

for fully stripped ions
A/Z selection

0.1 mm **ΔE Si-detector**
20 mm diameter

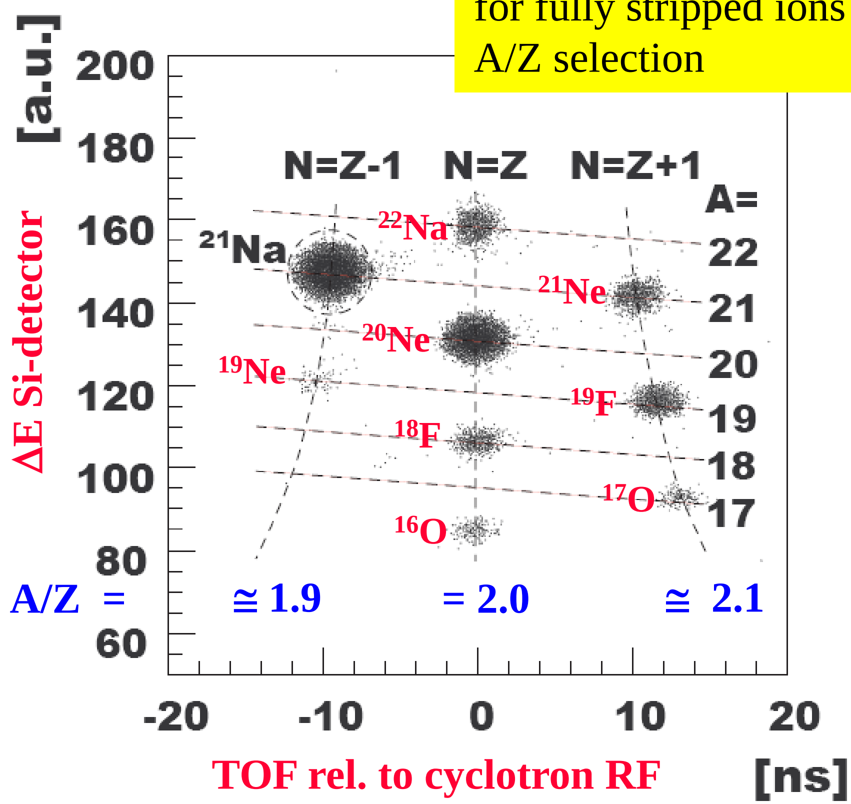

Example: Production of ^{21}Na via H(^{21}Ne,n)^{21}Na with $^{21}Ne^{7+}$ beam at 43MeV/nucleon using the TRIμP Separator, KVI Groningen
Ions after target fully stripped e.g. $^{21}Ne^{10+}$!

^{21}Ne beam with $\cong 10^{10}$ ions/s with $B\rho(^{21}Ne)/ B\rho(^{21}Na) \cong 1.09$ is all but eliminated by a slit (SH2) in front of plane I

Note:

Ions with A/Z ~ 2 are not separated !

Achromatic magnet separator with Wedge

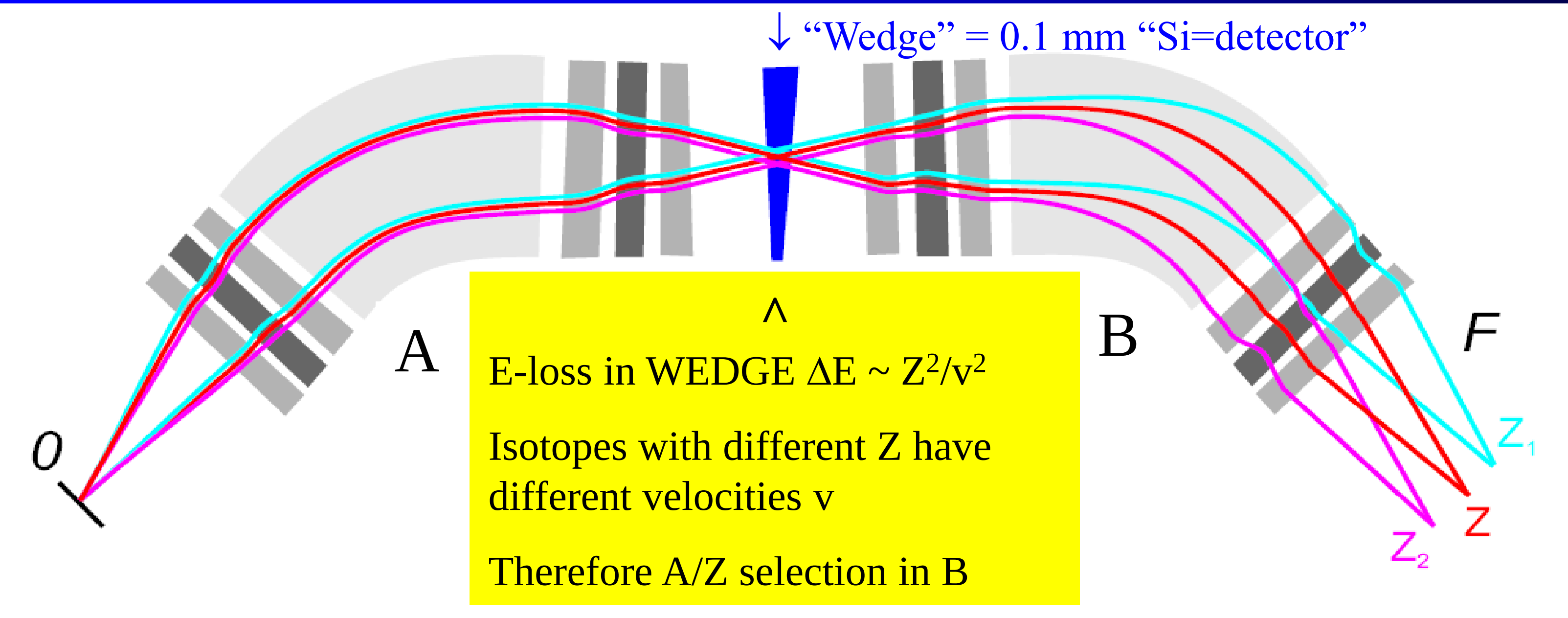

Figure from Experimental Techniques at NSCL, MSU, Th. Baumann, 8/2/2002

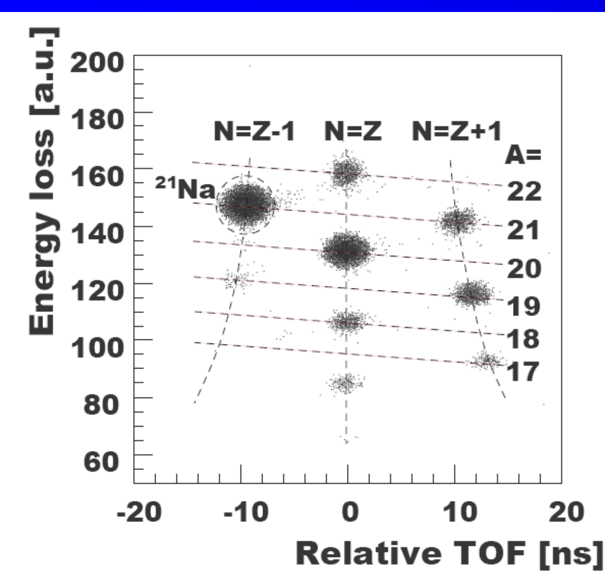

Effect of "Wedge" ⇒

Note:

For large dp/p) the degrader should be Wedge-shaped to restore achromaticity effected by degrader with constant thickness

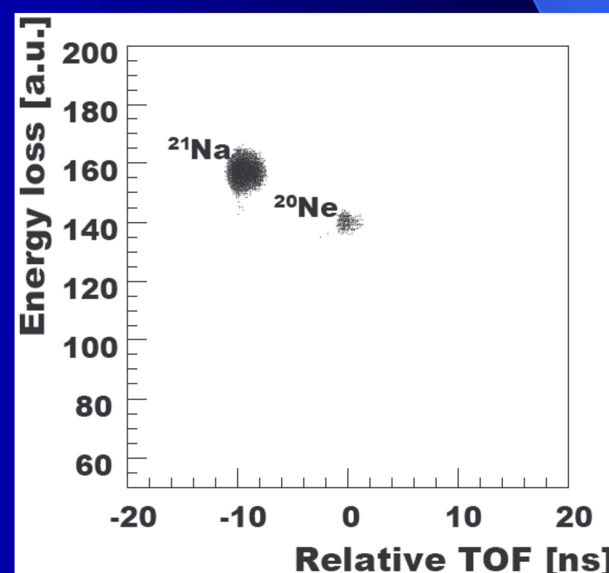

TRIμP an achromatic secondary beam separator

SH = Slits
Q = Quadrupoles
B = Dipoles

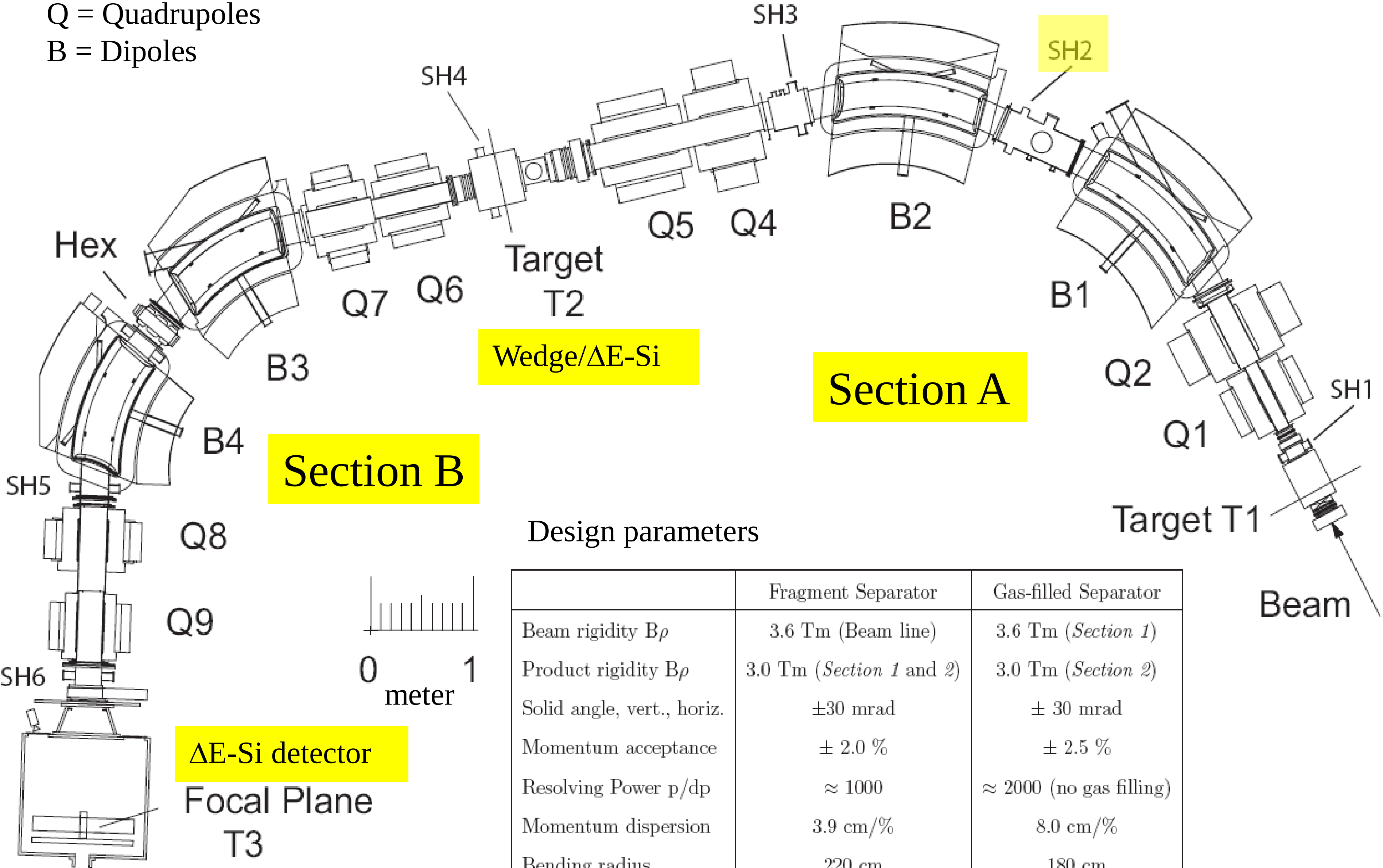

Design parameters

	Fragment Separator	Gas-filled Separator
Beam rigidity $B\rho$	3.6 Tm (Beam line)	3.6 Tm (*Section 1*)
Product rigidity $B\rho$	3.0 Tm (*Section 1* and *2*)	3.0 Tm (*Section 2*)
Solid angle, vert., horiz.	±30 mrad	± 30 mrad
Momentum acceptance	± 2.0 %	± 2.5 %
Resolving Power p/dp	≈ 1000	≈ 2000 (no gas filling)
Momentum dispersion	3.9 cm/%	8.0 cm/%
Bending radius	220 cm	180 cm

TRIμP ion-optics

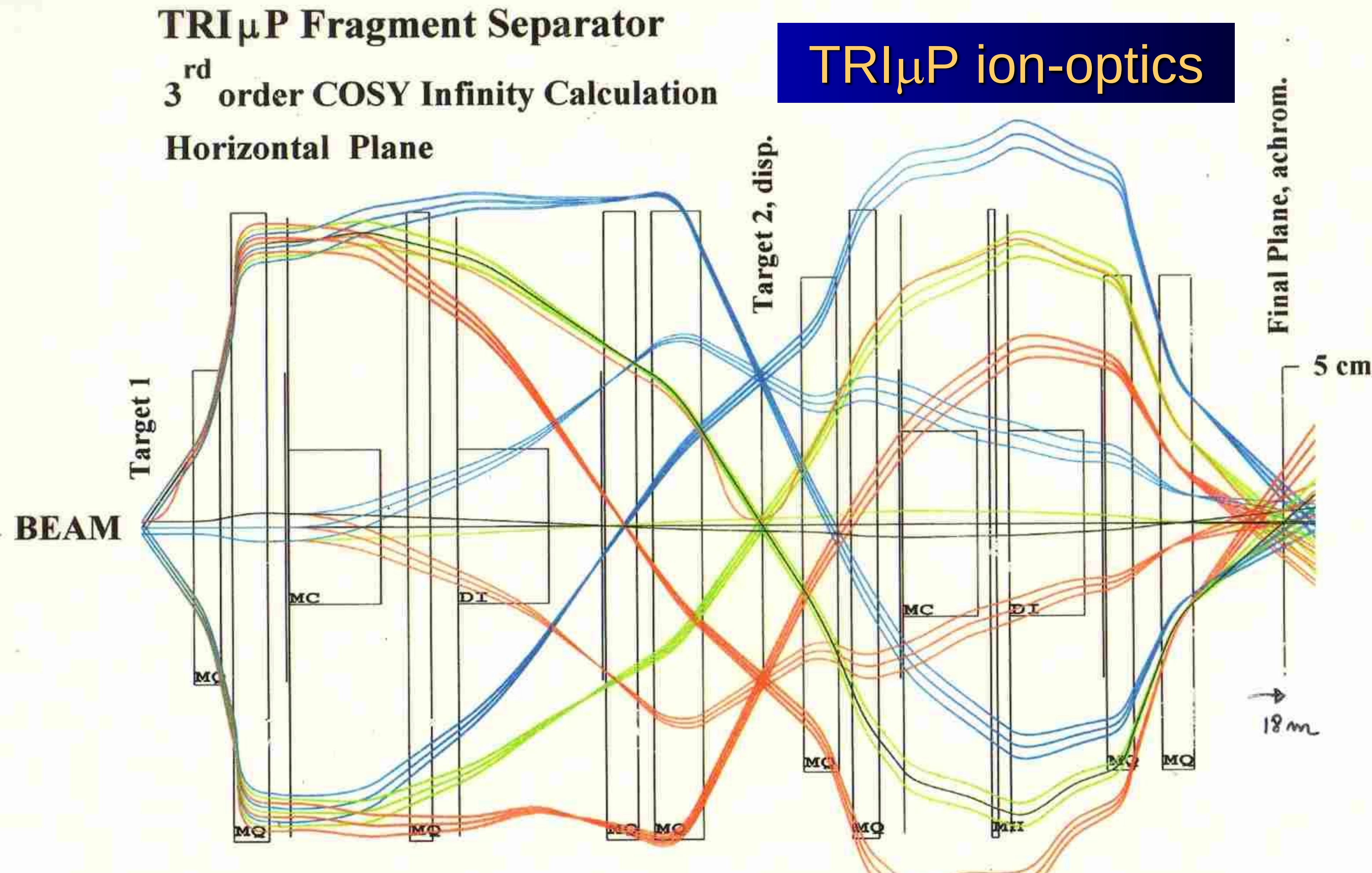

Ray Definitions at Target

x = +/- 2 mm

θ = +/- 30 mrad

dp = +/- 2.5 %

A1900 MSU/NSCL Fragment Separator

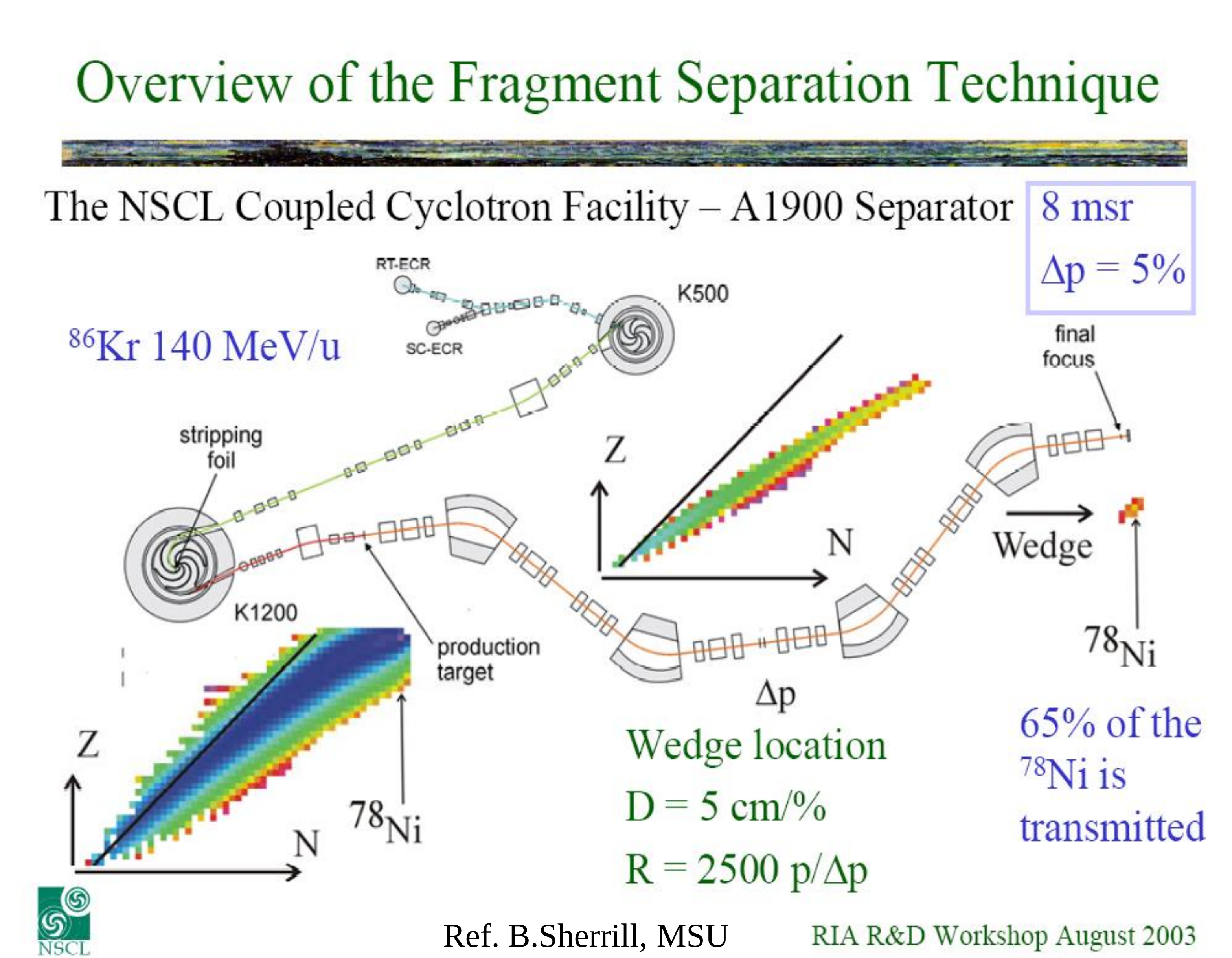

Another example are the BigRIPS Fragment Separator at RIKEN in Japan And the Super-FRS at GSI.

Gas-filled separators Concept

PROBLEM: After target, a distribution of several charge states q exists for low E or large Z, with Bρ range typically larger than acceptance causing transmission losses.

REMEDY: gas-filled separator

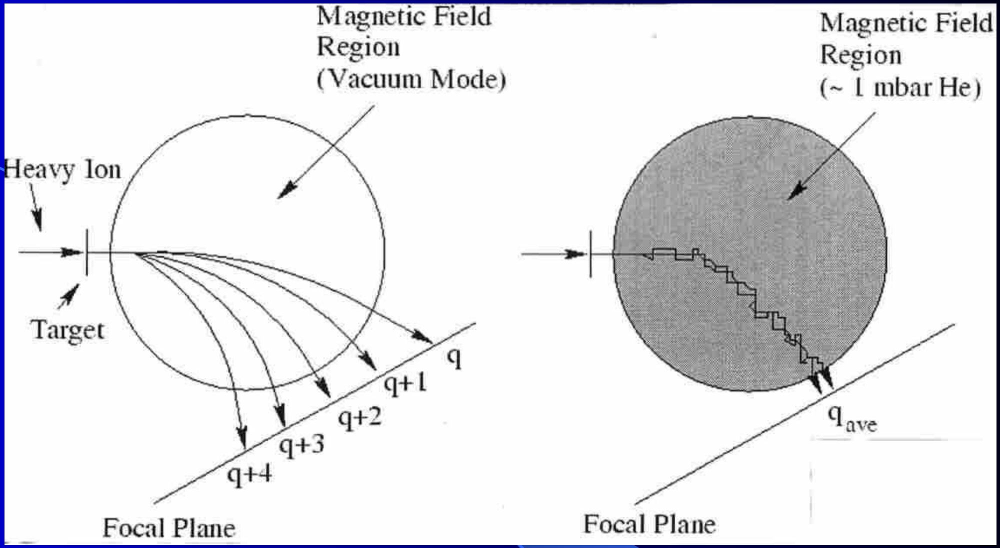

Rays in a magn. dipole field without and with gas-filling

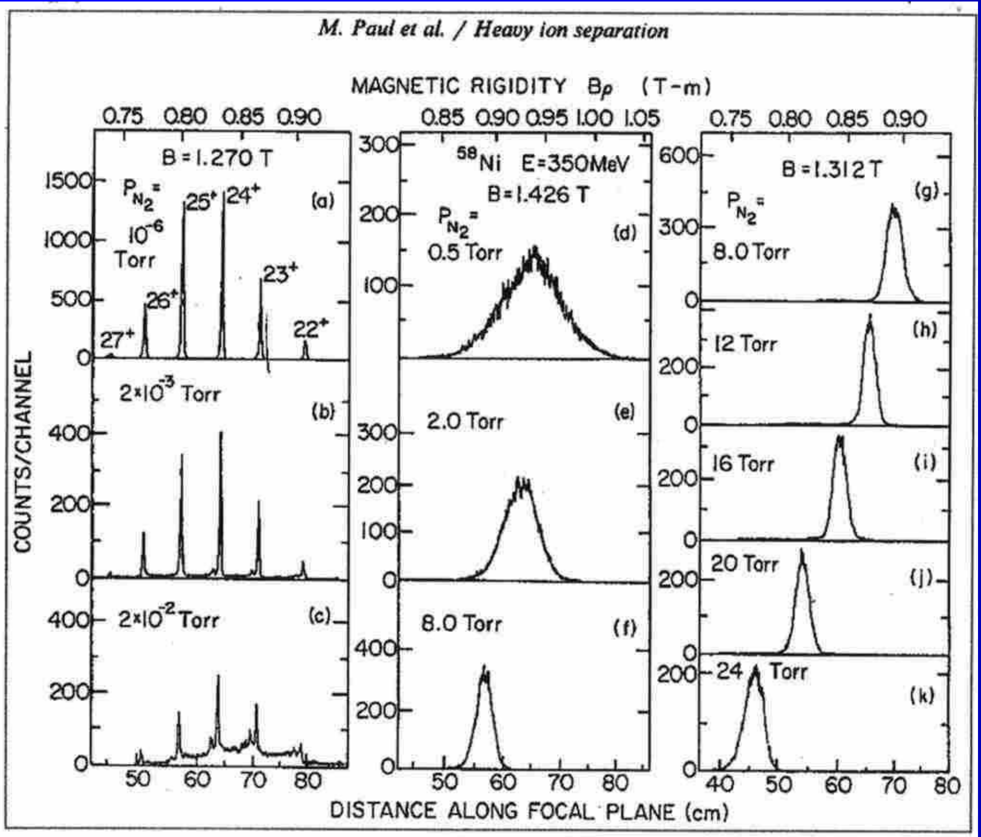

Measured spectra as function of gas pressure (e.g. He, Ar)

M. Paul et al. NIM A 277 (1989) 418

TRIμP ion-optics Section B

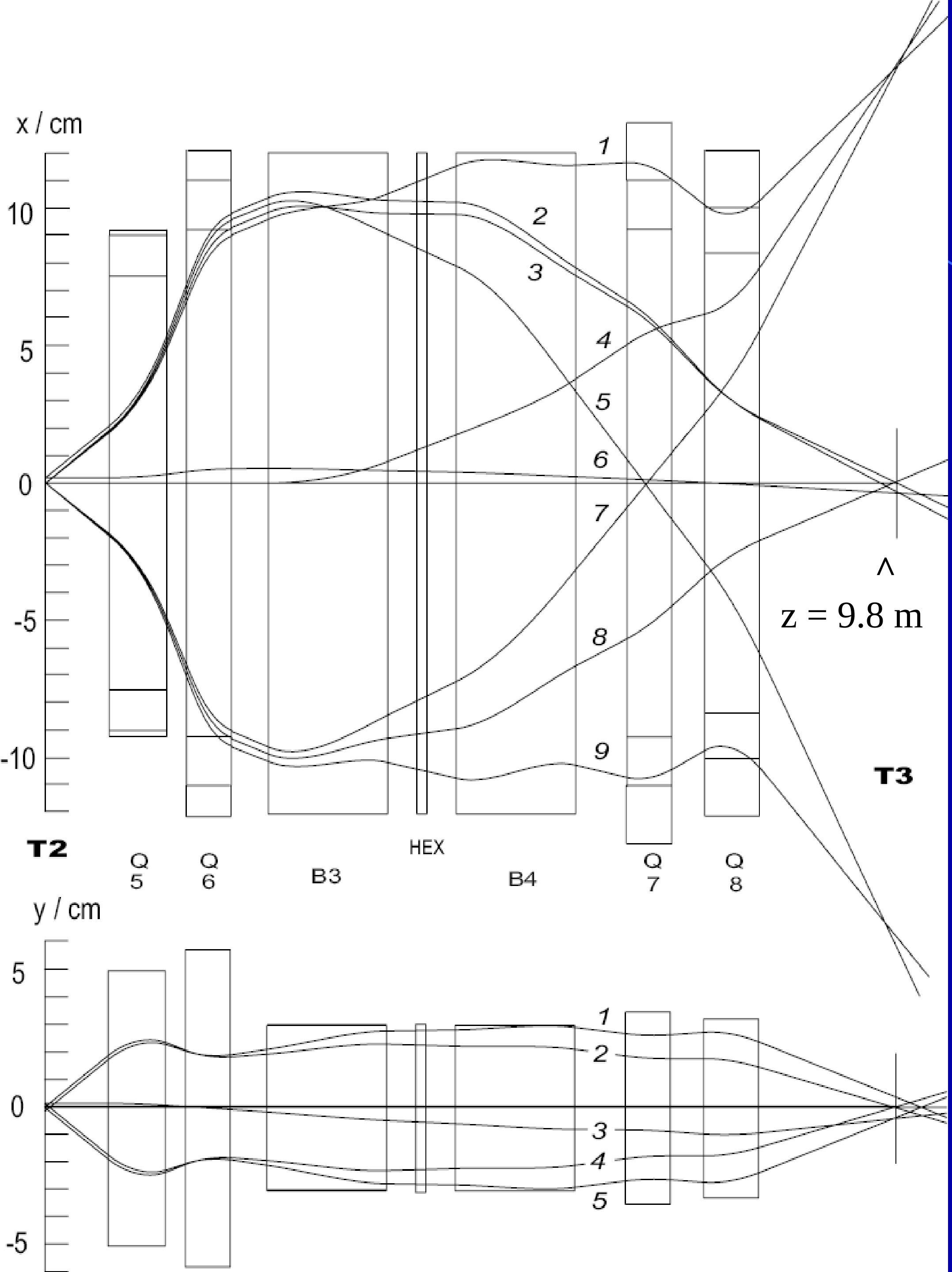

A "long" achromatic separator system is not suitable for a gas-filled separator that should be "short" to reduce statistical E spread and have "large dispersion"

ray	x [mm]	Θ [mrad]	ΔE/E [%]	y [mm]	Φ [mrad]
1	0	30	4.0	-1.5	30
2	2	30	0	0	30
3	0	30	0	1.5	0
4	0	0	4.0	0	-30
5	0	30	-4.0	1.5	-30
6	2	0	0		
7	0	-30	4.0		
8	0	-30	0		
9	0	-30	-4.0		

Therefore:

The TRIμP separator was Designed to be able operate with Section A as beam line & Section B as short gas-filled separator with large dispersion

Charge state distribution in TRIμP separator with gas-filling

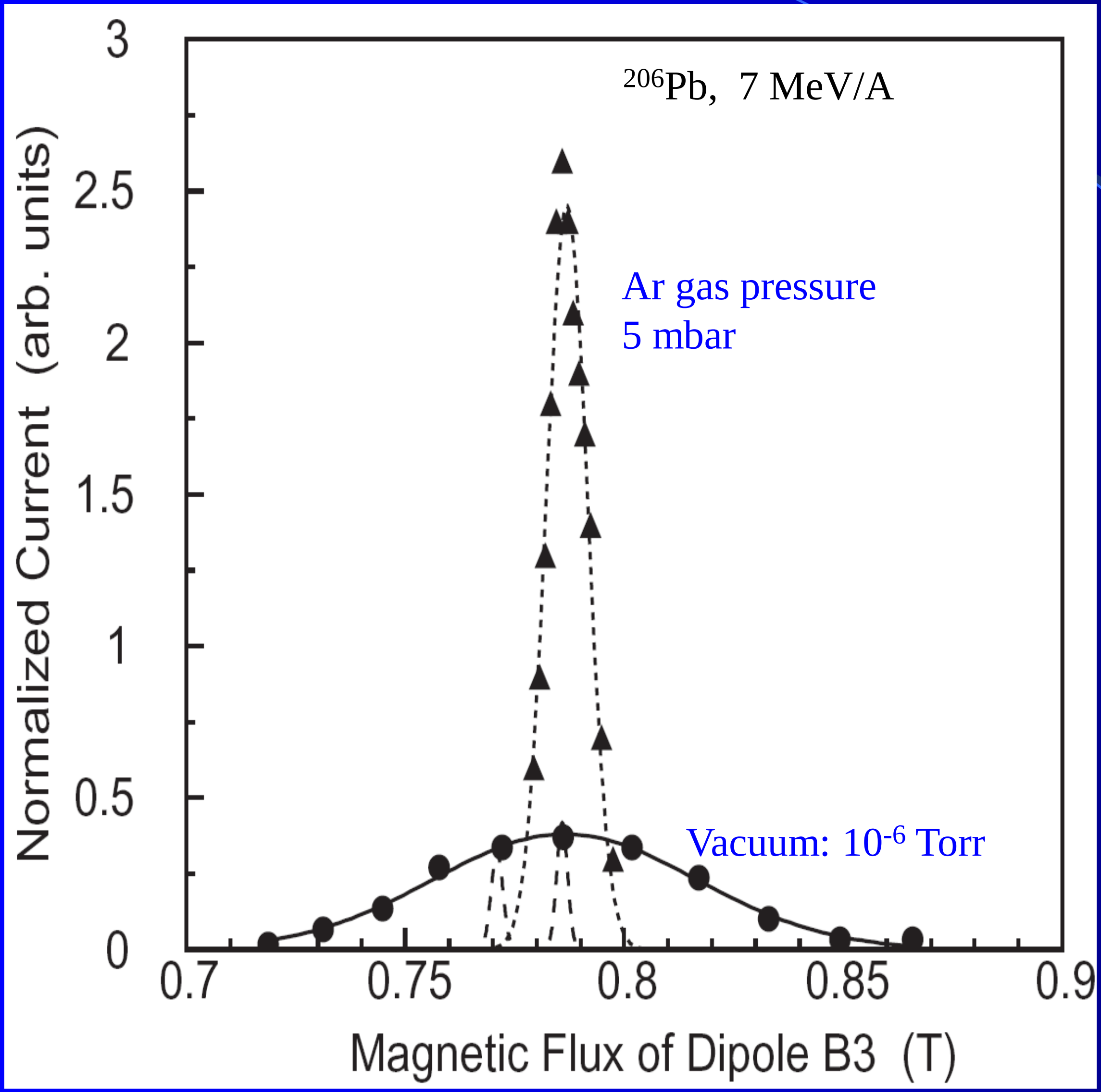

Difference between Fragment and Recoil Separators

- Fragment separators use high energy beams to produce efficiently rare isotopes (RI).

- Recoil separators work at low energy to study astrophysical reactions.

CONSEQUENCES:

- Fragment separators use the ΔE loss in Wedges to separate RIs.

- Recoils separators use Electric fields to separate beam and recoils due to their mass differences. Either electric dipoles or Wien filters.

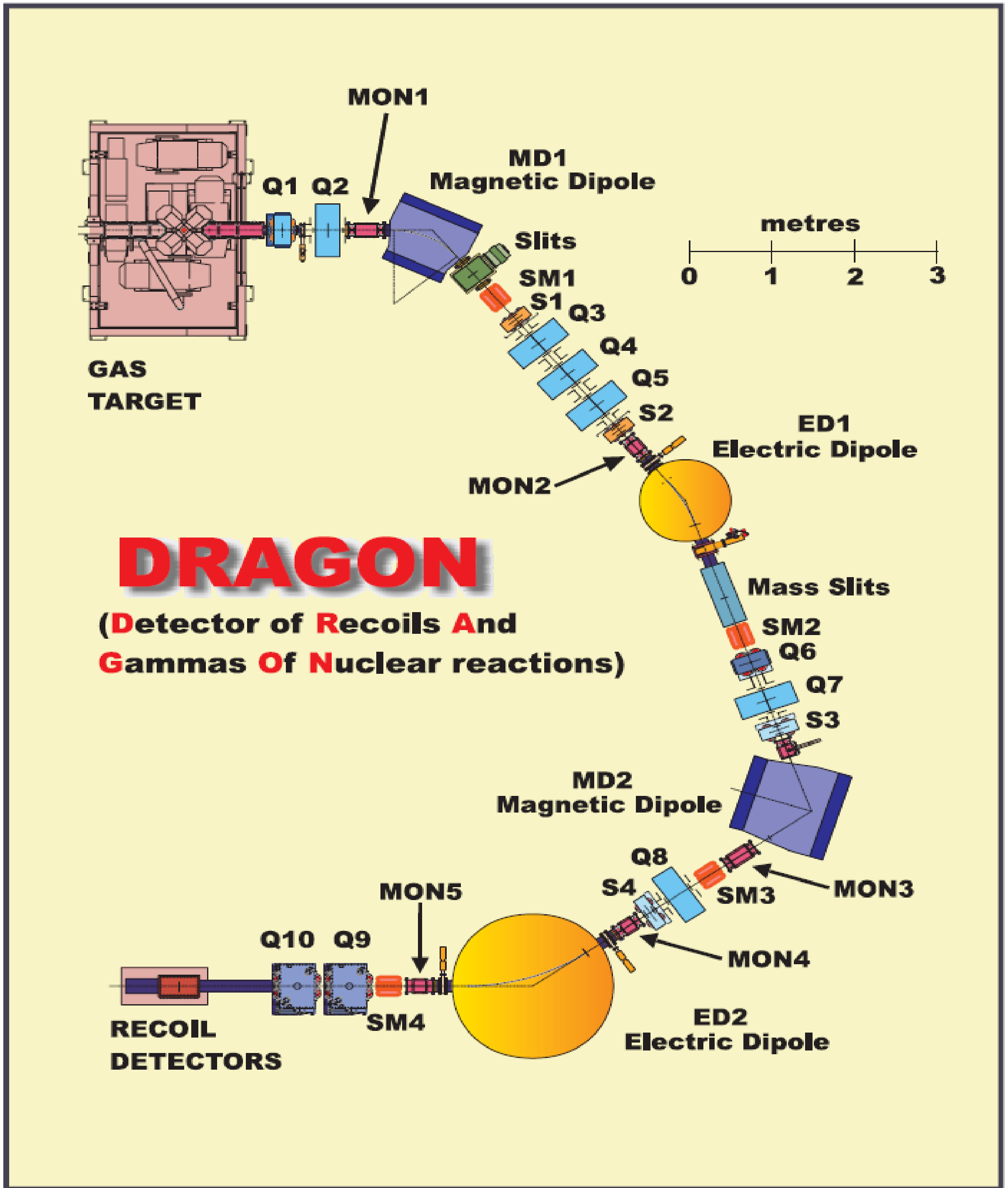

DRAGON

Recoil Separator with Electric Dipoles

Study of astrophyscis reactions using radioactive beams:

e.g. $^{21}Na(p,\gamma)^{22}Mg$ in inverse kinematics using a radioactiv ^{21}Na beam of 4.62 MeV to study NeNa cycle

Ref. Dragon Recoil Separator Optics, The Recoil Group, 1/18/1999,TRIUMF

DRADON Ion-optics

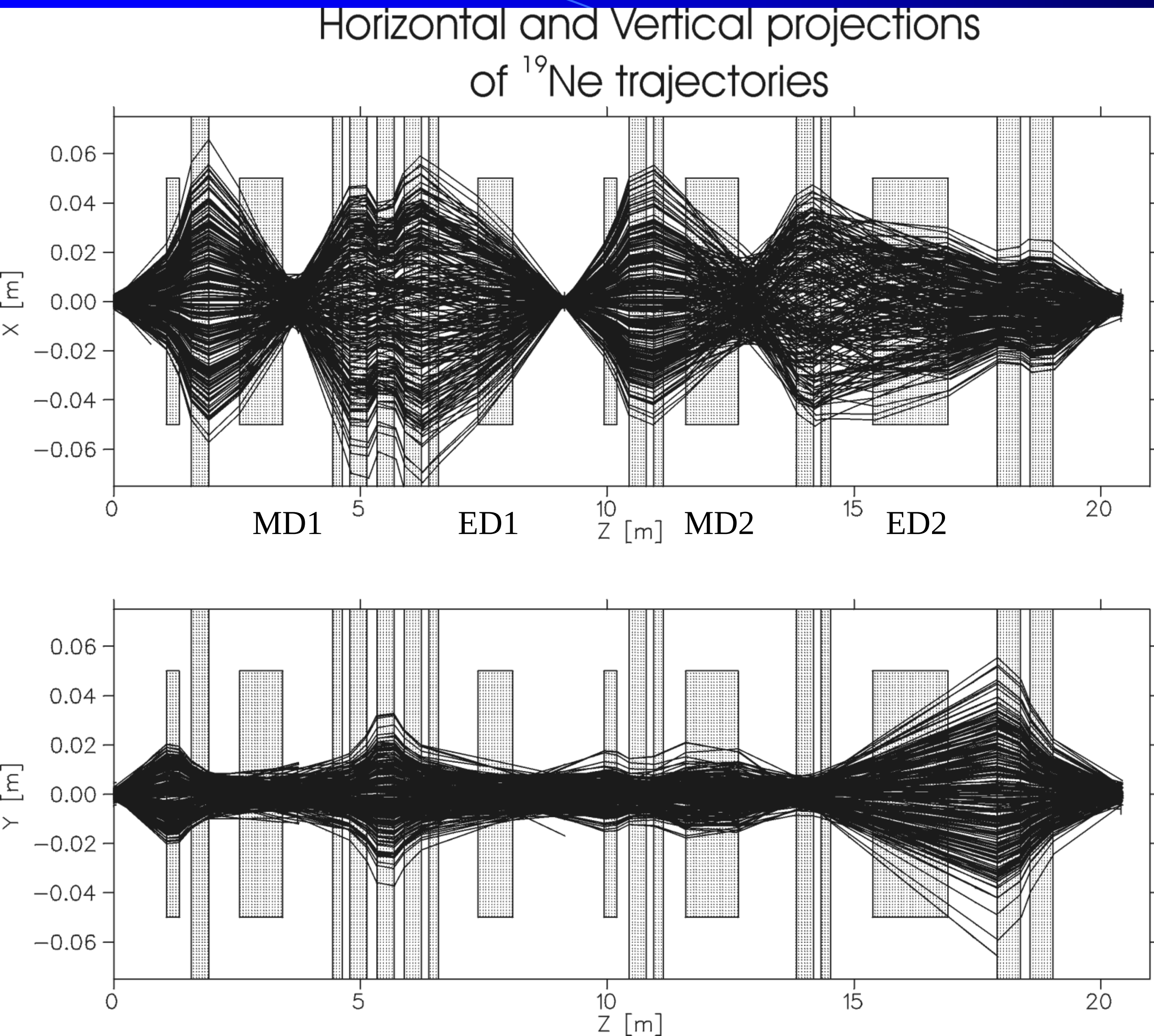

Ref. J. M. D'Auria et al.
TRIUMF

EMMA
Recoil Separator for ISAC-II at TRIUMF

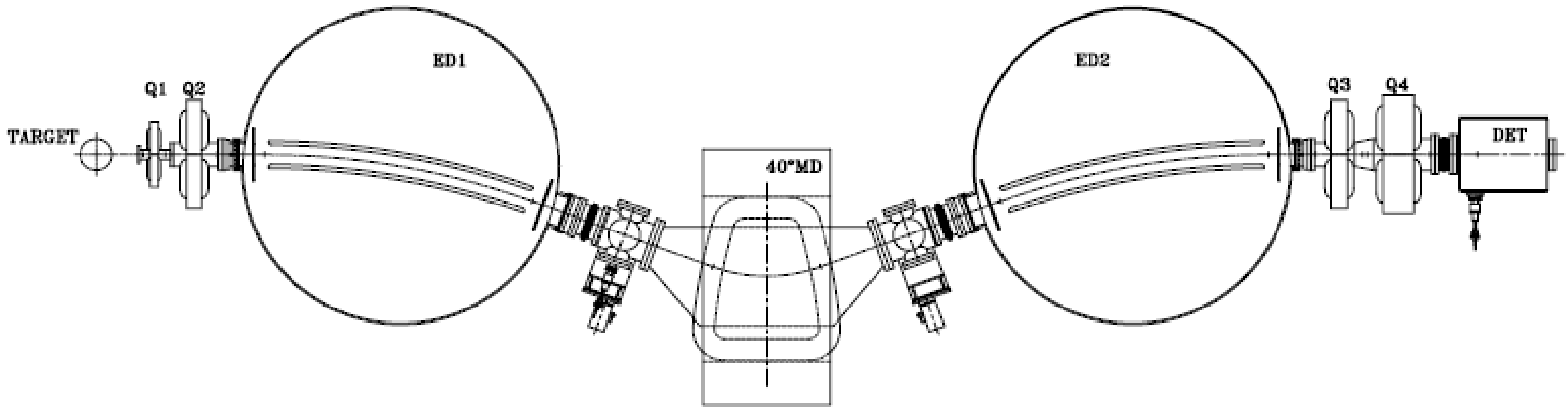

Fig. 1. Schematic view of EMMA, showing the target, quadrupole and dipole magnets, and electric dipoles. The detector box is also indicated.

B. Davids, TRIUMF &
C. Davids, ANL

ERNA

Recoil Separator with Wien Filters

Study of the astrophysicial reaction $^{12}C(\alpha,\gamma)^{16}O$ in inverse kinematics $^{4}He(^{12}C,\gamma)^{16}O$ at E_{cm} = 0.7 MeV

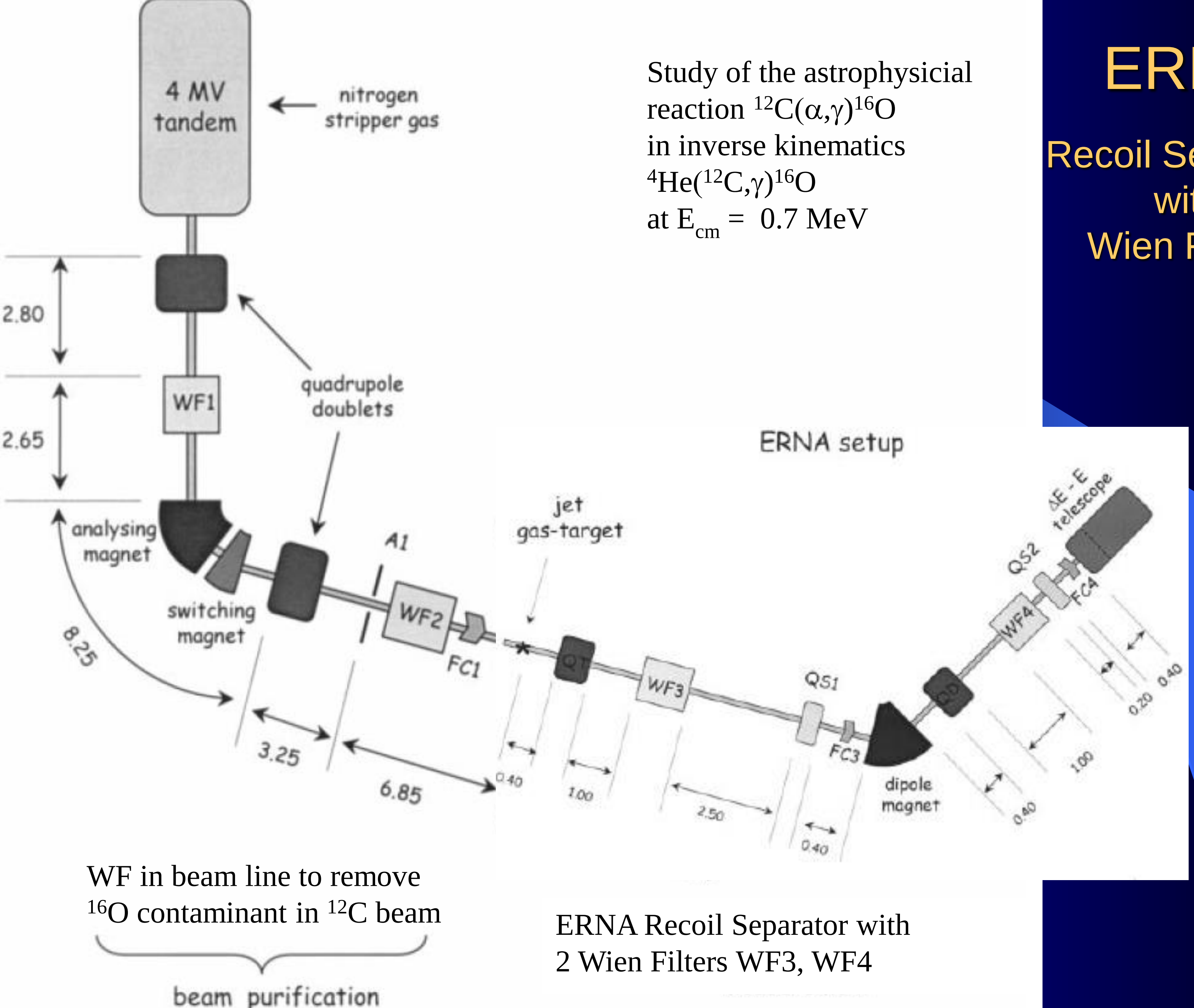

WF in beam line to remove ^{16}O contaminant in ^{12}C beam

ERNA Recoil Separator with 2 Wien Filters WF3, WF4

ERNA

Recoil Separator with Wien Filters

Ion-optics of ^{16}O 3^+ and 6^+ ions

3rd order calculations using COSY Infinity

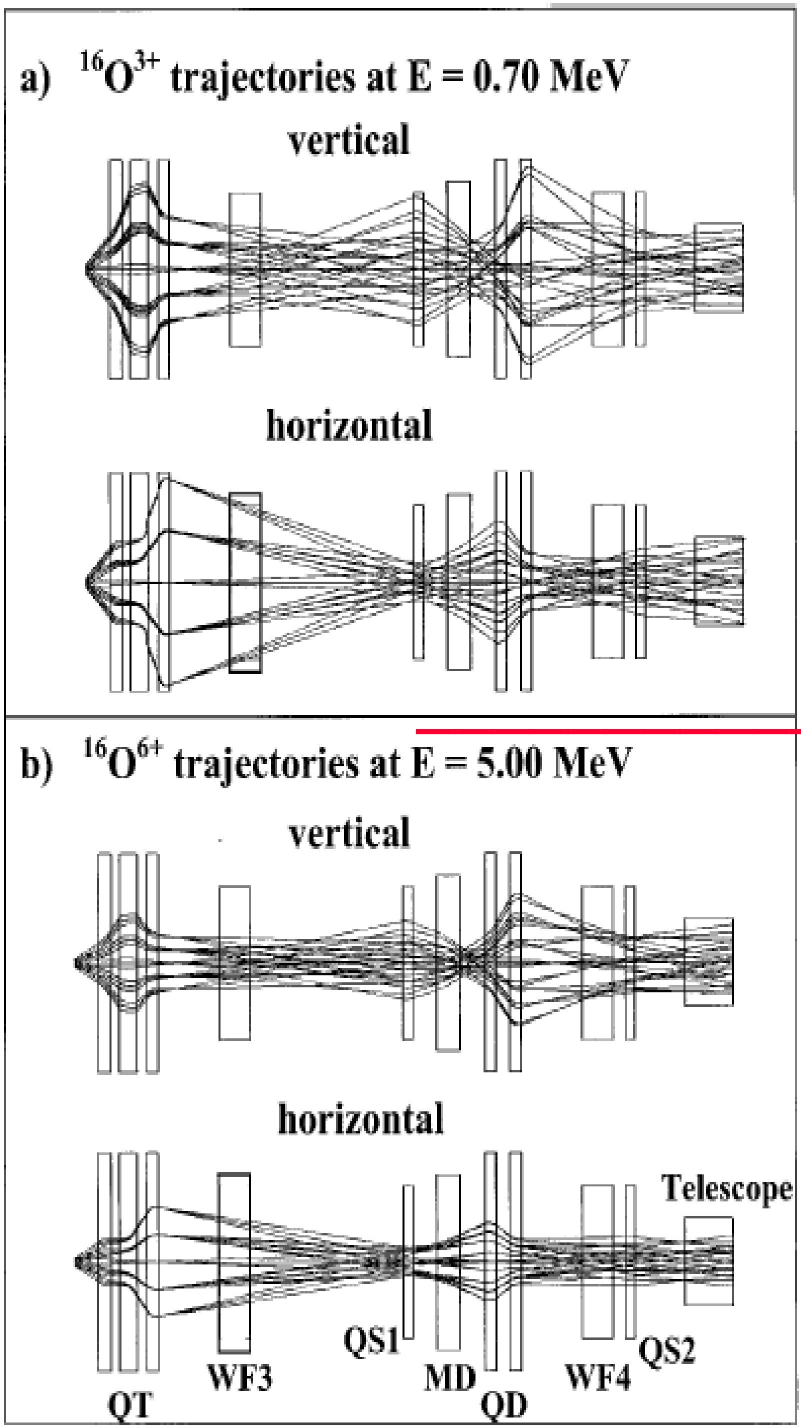

^{12}C beam mainly stopped in Faraday cup between QS1 and MD

Fig. 2. Samples of ^{16}O trajectories are shown for (a) E = 0.70 MeV ($q_0 = 3^+$, $\theta_{max} = 1.9°$, ΔE = 0.13 MeV) and (b) E = 5.0 MeV ($q_0 = 6^+$, $\theta_{max} = 1.0°$, ΔE = 0.44 MeV). The trajectories start at the jet gas-target (^4He target density $= 1 \times 10^{18}$ atoms/cm^2) and are followed through the filtering and focusing elements of ERNA (indicated by square boxes) up to the telescope (WF = Wien filter, QS = quadrupole singlet, QD = quadrupole doublet, QT = quadrupole triplet, MD = magnetic dipole)

Study of astrophyscis reactions using radioctive beams.

ARES

Recoil Separator with a Wien Filter

Example: Hot CNO breakout reaction $^{19}Ne(p,\gamma)^{20}Na$ in inverse kinematics using a radioactive ^{19}Ne beam of 10.1 MeV

Ref. M. Couder, PhD Thesis July 2004, Louvain-La-Neuve

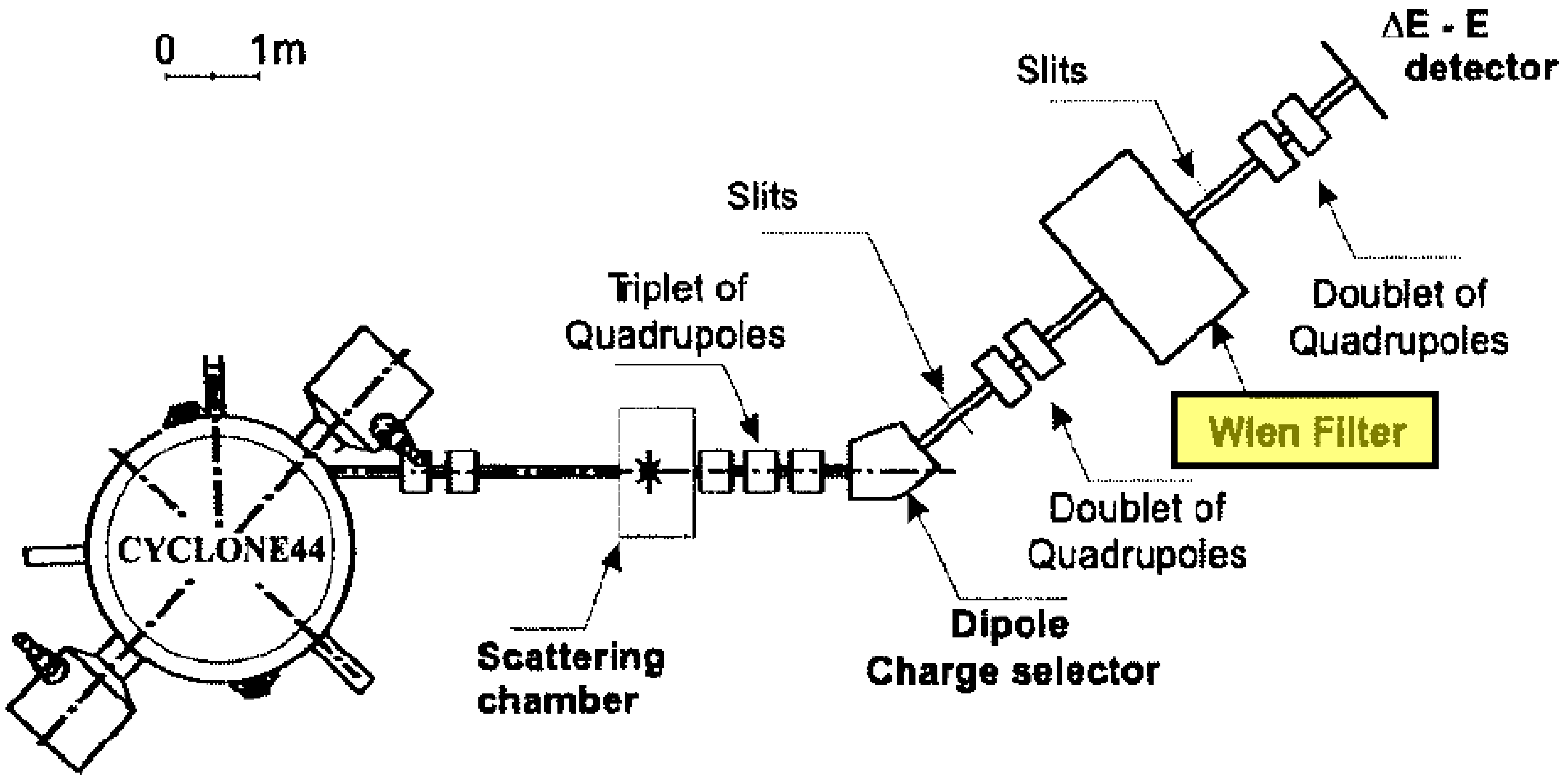

Recoil Separator St. George

Study of (α,γ) [and (p, γ)] of astrophysics importance,
for A < ≈ 40 targets,
emphasis on low energies, i.e. very small cross sections,
max. energy of 4 MeV/A

An overview of reaction result in the following
DESIGN PARAMETERS

Maximum magnetic rigidity Bρ:	0.45 Tm
Minimum magnetic rigidity Bρ:	0.10 Tm
Momentum acceptance dp:	+/- 3.7 %
Angle acceptance, horiz & vert.:	+/- 40 mrad

Further design considerations:

- Two phase construction
- Charge selection by Bρ analysis (typical: 50% Transmission)
- High mass resolution (Δm/m ≅ 100, 1st phase with 2 Wien Filters)
- Higher mass resolution (Δm/m ≅ 600) 2nd phase
- Wien Filters for mass resolution (energy too low for “Wedge” method)

St. George, Layout

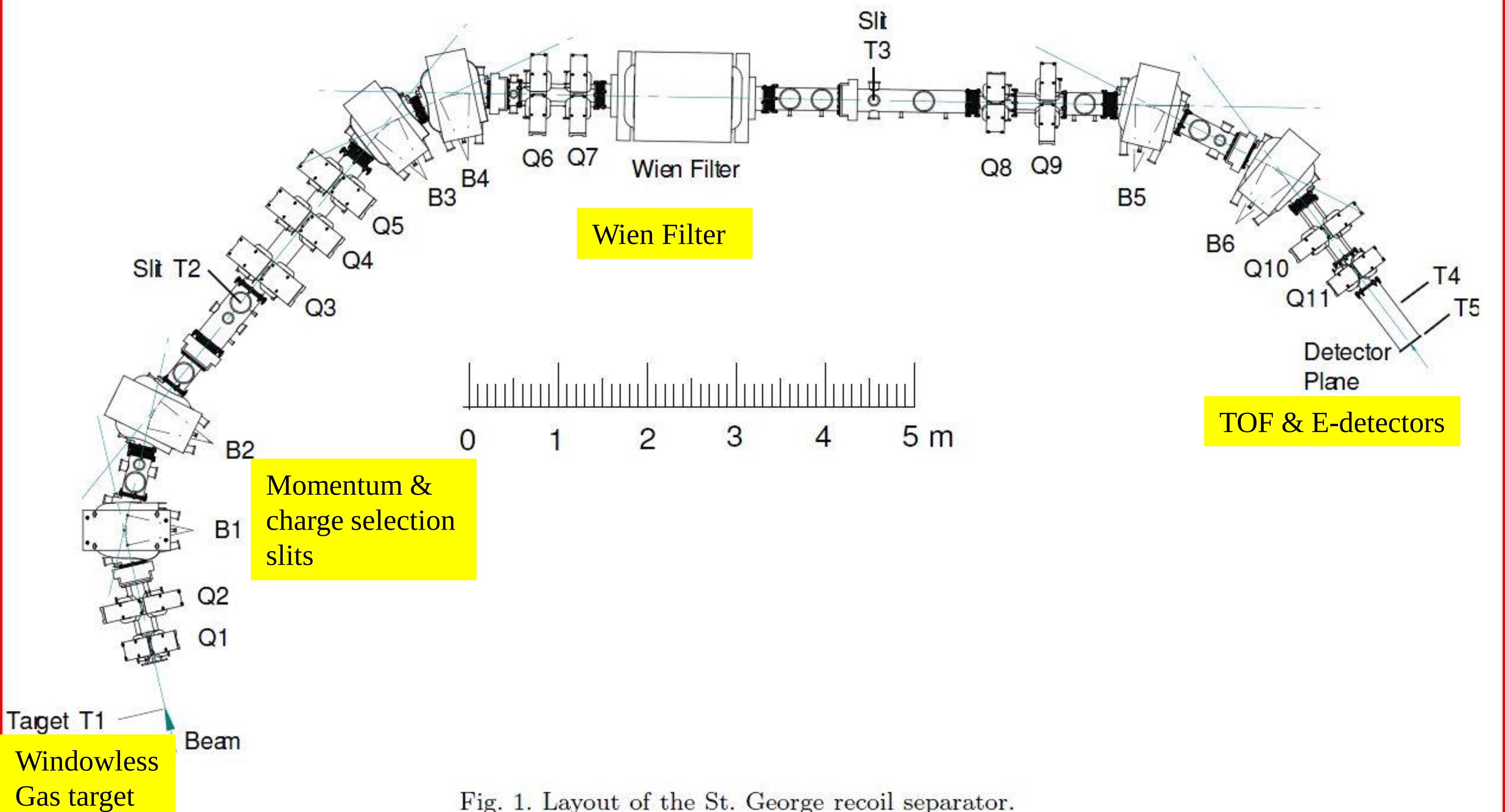

Fig. 1. Layout of the St. George recoil separator.

The Wien Filter

$$\vec{F} = q\vec{E} + q\vec{v} \times \vec{B}$$

Electric force — Magnetic force

(1)

$F = 0$ when $qE = qv \times B$ with $E \perp B$

$v = E/B$ with $E \perp B$ **(22)**

$v \neq E/B$
$F = (m/q)a = E+vB)$
a = acceleration
Leads to m/q separation
Select q before Wien Filter

Design study of Wien Filter for St. George

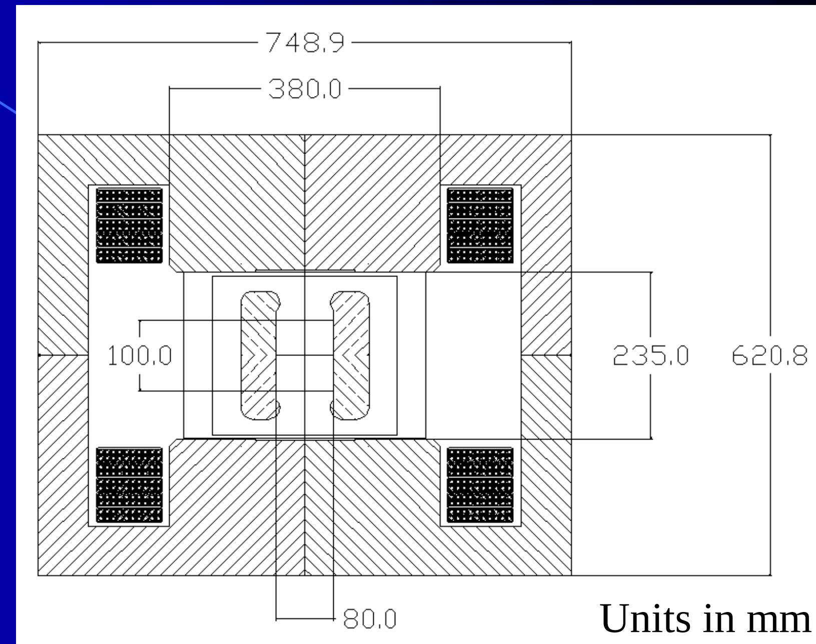

Electrostatic system of Danfysik Wien Filter

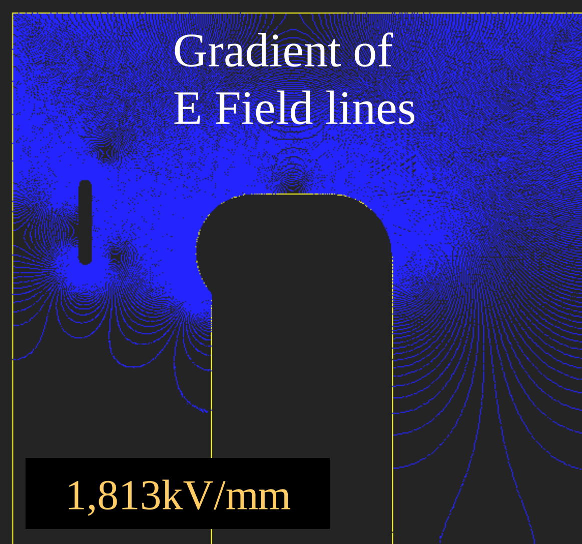

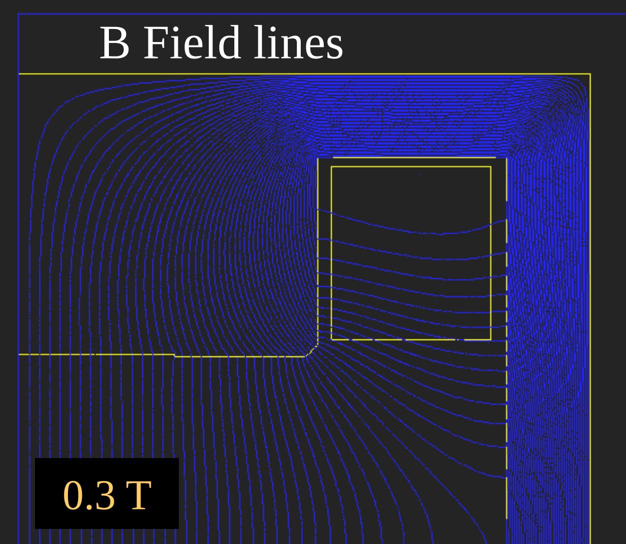

St. George Ion-optics

Characteristic rays

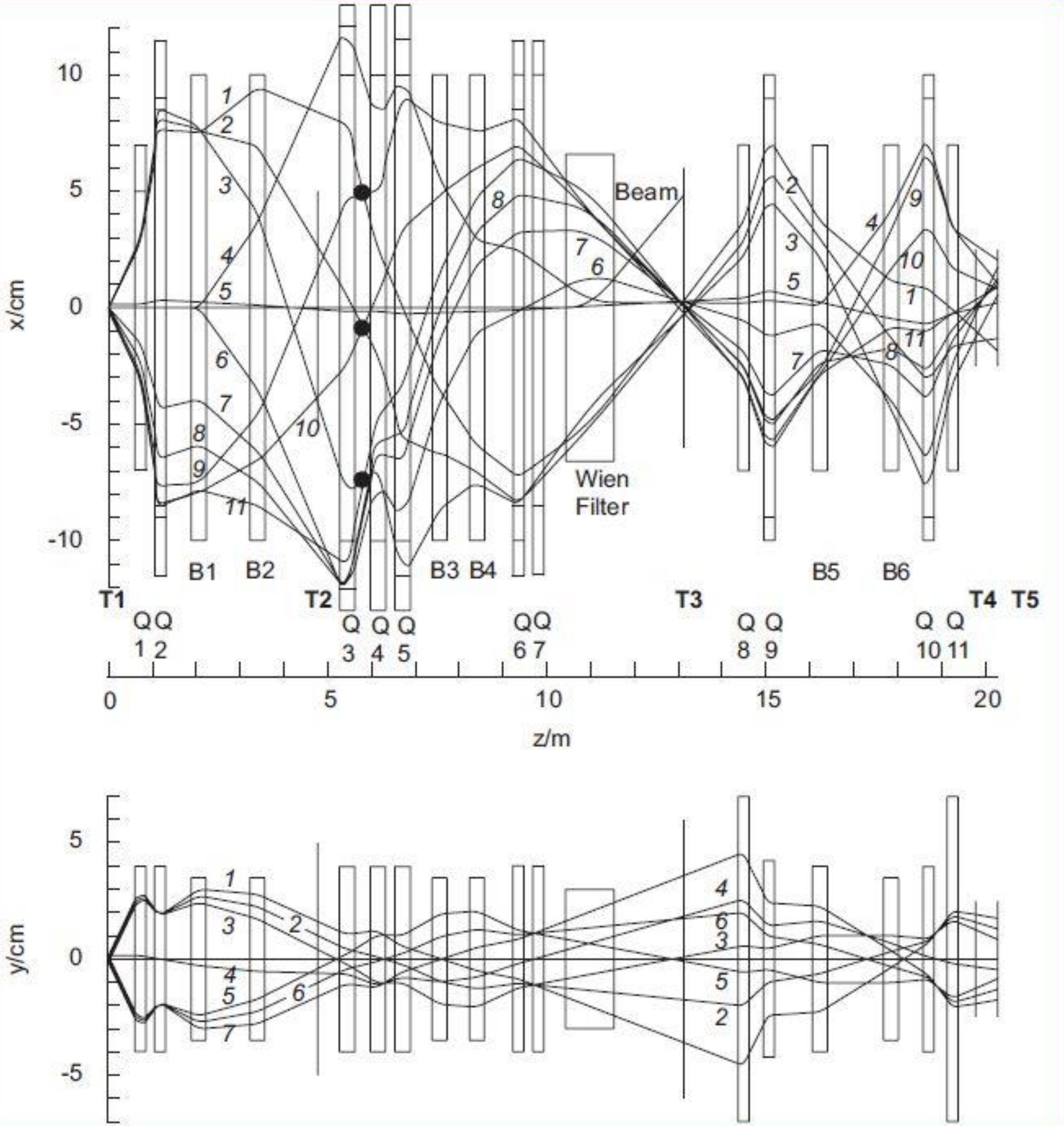

St. George, Envelope

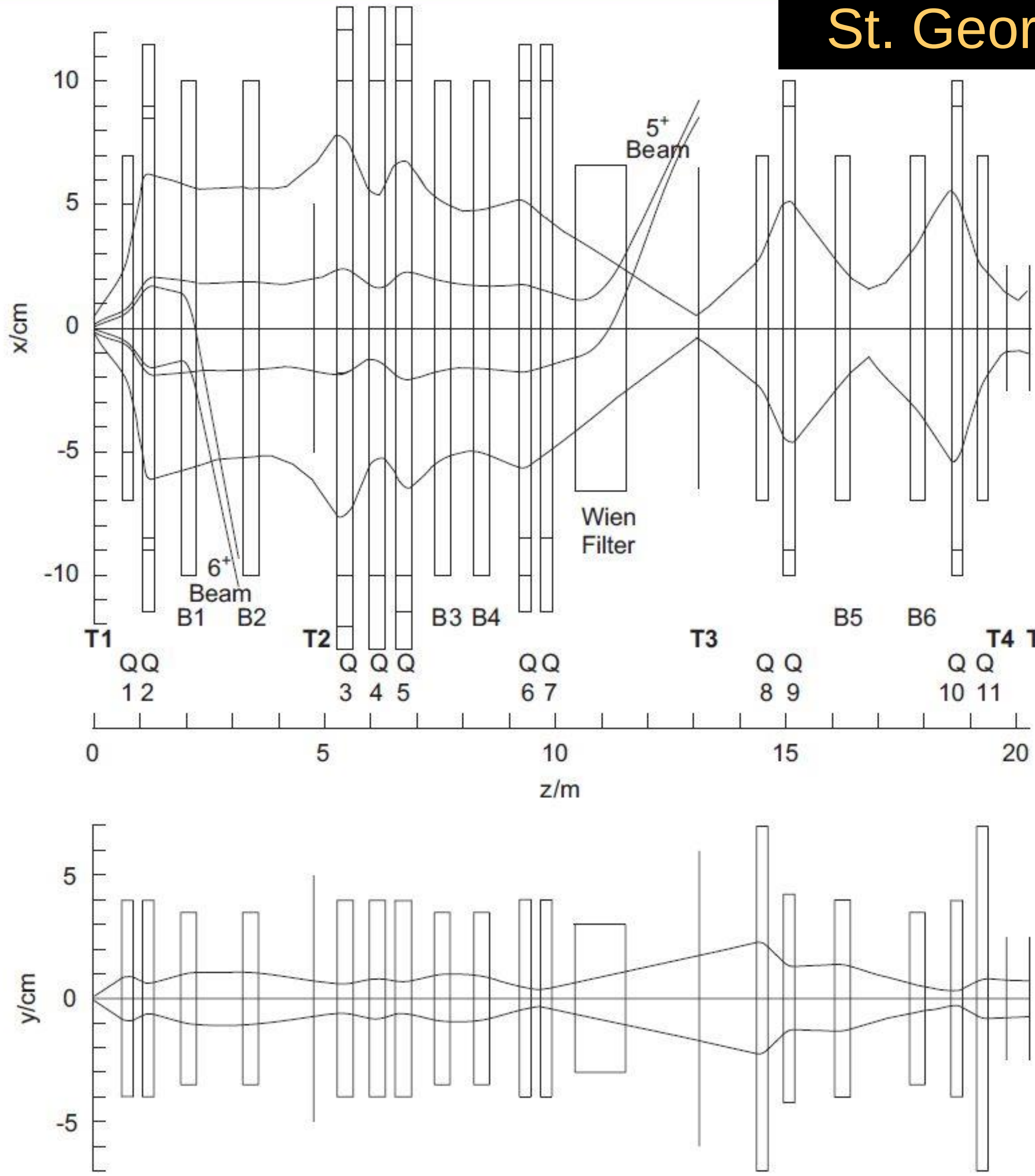

Fig. 3. Ion optics of the $^{22}Ne(\alpha,\gamma)^{26}Mg$ reaction in inverse kinematics at 4.6 MeV incident energy. Shown are the horizontal envelopes of the 5^+ reactio[n] products, and the most abundant 5^+ and the 6^+ beams. The lower panel shows the vertical envelope of the reaction products.

St. George Wien Filter (velocity filter)

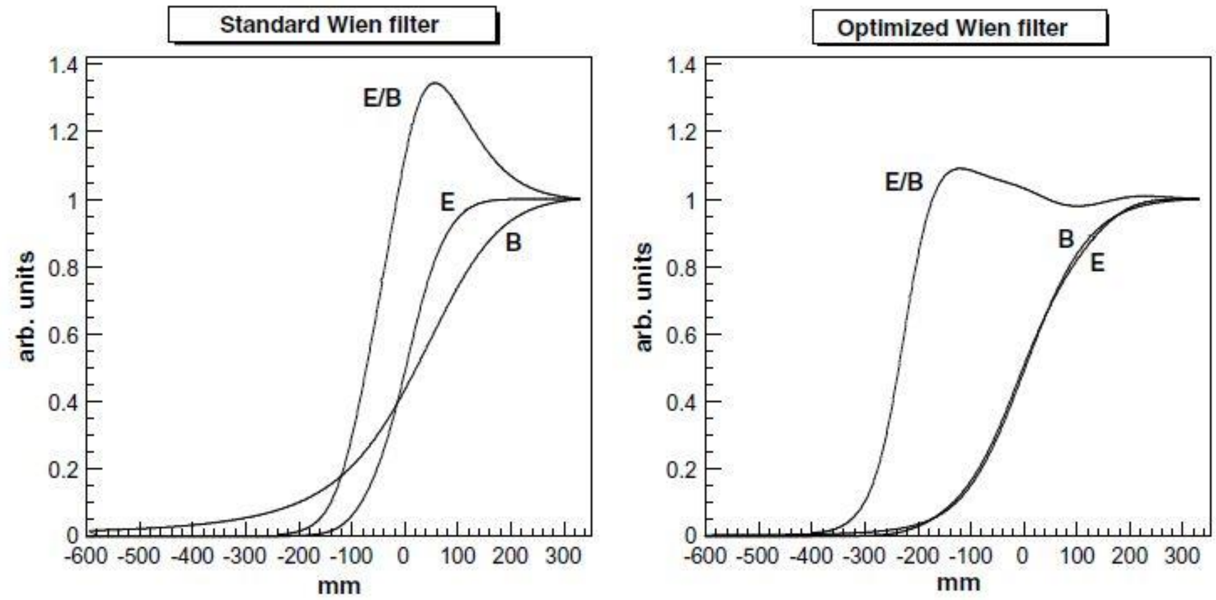

Fig. 3. Fringe field comparison of a standard Wien filter (left panel) and the newly designed (right panel). The ratio of the fields is also shown.

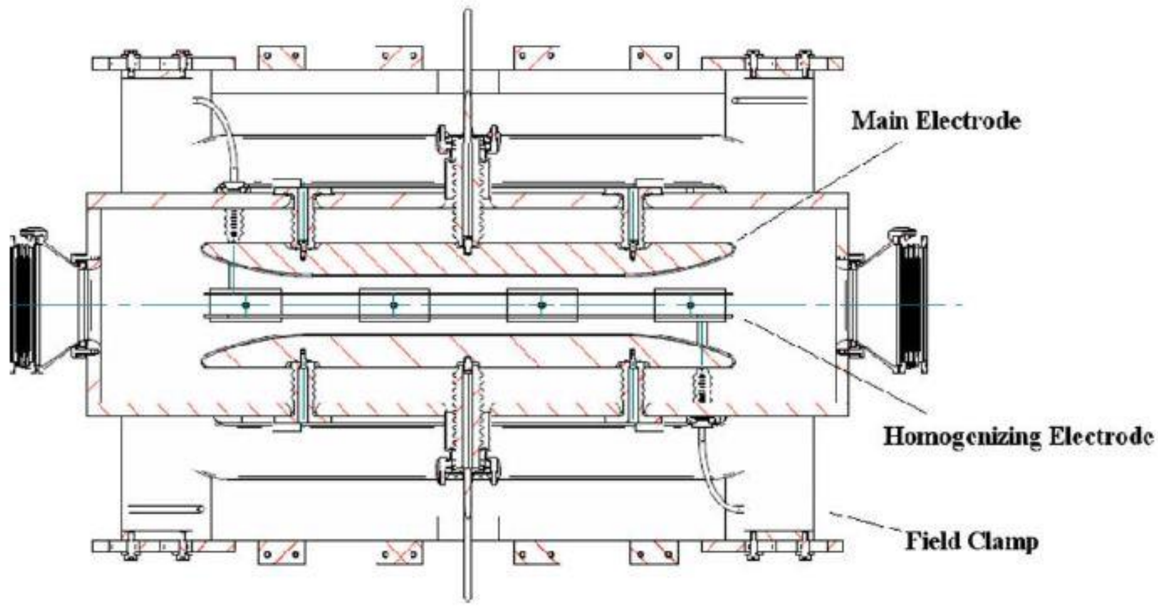

Fig. 4. A top view of the horizontal midplane of the Wien filter is shown. Electrostatic dipole is mounted inside the magnet.

SECAR

- SECAR radiative capture on unstable beams, can only be measured in inverse kinematics
- Designed to make use of high-intensity FRIB beams
- Up to masses A = 65 to cover the expected mass range of the rp process, (p, γ)
- Beam rejection 10^{17} , therefore mass separation m/dm > 750
- 4 ion-optical sections, charge selection, first Wien Filter, second Wien Filter, clean-up section
- Energy range E_{cm} = 0.2 – 3 MeV

Broad Set of Reactions Define Rigidity and Acceptance Parameters

Charge B

Reaction	E_{cm} Beam MeV	Q-value MeV	dE/E Range %	Recoil Charge q	Half Angle, Recoil mrad	$B\rho$ Recoil Tm	$E\rho$ Recoil MV	$B\rho$ Beam Tm
$^{15}O(\alpha,\gamma)^{19}Ne$	0.5	3.529	±3.1	3	±15.6	0.29	1.25	0.14
	3	3.529	±2.1	6	±10.3	0.35	3.75	0.35
$^{44}Ti(\alpha,\gamma)^{48}Cr$	0.5	7.696	±2.3	4	±11.7	0.58	2.74	0.19
	3	7.696	±1.3	10	±6.2	0.57	6.59	0.48
$^{19}Ne(p,\gamma)^{20}Na$	0.2	2.193	±1.3	4	±6.4	0.31	1.88	0.21
	3	2.193	±0.71	9	±3.6	0.54	12.5	0.81
$^{23}Mg(p,\gamma)^{24}Al$	0.2	1.872	±0.92	4	±4.6	0.38	2.28	0.15
	3	1.872	±0.56	11	±2.8	0.53	12.4	0.58
$^{25}Al(p,\gamma)^{26}Si$	0.2	5.517	±2.3	4	±11.7	0.41	2.48	0.15
	3	5.517	±0.90	11	±4.5	0.58	13.5	0.58
$^{30}P(p,\gamma)^{31}S$	0.2	6.133	±2.2	4	±10.8	0.49	3.97	0.15
	3	6.133	±0.80	12	±4.0	0.63	14.8	0.58
$^{33}Cl(p,\gamma)^{34}Ar$	0.2	4.663	±1.5	5	±7.6	0.43	2.6	0.31
	3	4.663	±0.6	14	±3.1	0.59	14.0	1.19
$^{34}Cl(p,\gamma)^{35}Ar$	0.2	5.897	±1.8	5	±9.2	0.44	2.7	0.32
	3	5.897	±0.7	14	±3.5	0.61	14.4	1.22
$^{37}K(p,\gamma)^{38}Ca$	0.2	4.548	±1.3	5	±6.6	0.48	2.9	0.27
	3	4.548	±0.54	15	±2.7	0.62	14.6	1.04
$^{38}K(p,\gamma)^{39}Ca$	0.2	5.763	±1.6	5	±8.1	0.49	3.0	0.27
	3	5.763	±0.61	15	±3.1	0.64	15.0	1.06
$^{65}As(p,\gamma)^{66}Se$	0.2	2.030	±0.35	6	±1.8	0.70	4.3	0.18
	3	2.030	±0.21	21	±1.0	0.77	18.4	0.71

- These reactions define the following required design parameters
  - Even at highest energy most beams can be used for setup of experiments with sufficient count rate
  - Otherwise less-abundant higher charge states can be used

Min. - Max. Bρ 0.14- 0.80 Tm
Min. – Max Eρ 1.0 – 19 MV

Angle Accept., x, y +/- 25 mrad
Energy Acceptance +/- 3.1 %

SECAR Layout

Charge B

- SECAR consists of:
  - 2 Velocity filters (VF1, VF2)
  - 8 Dipole magnets
  - 14 Quadrupoles
  - 1 Quadrupole + Hexapole Q1(+Hex)
  - 3 Hexapoles
  - 1 Octupole

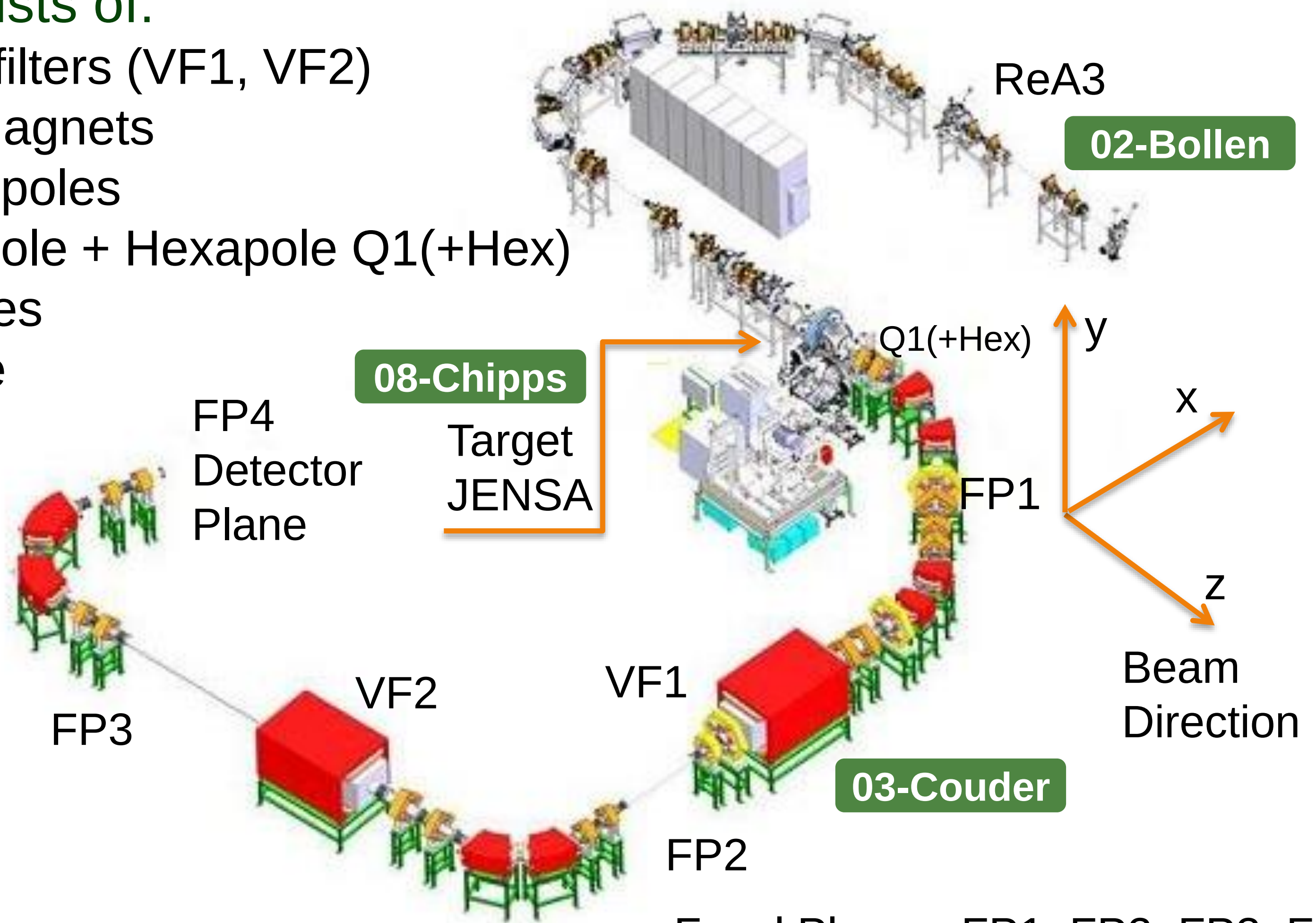

Focal Planes: FP1, FP2, FP3, FP4

SECAR Recoil Separator for Astrophysical Capture Reactions

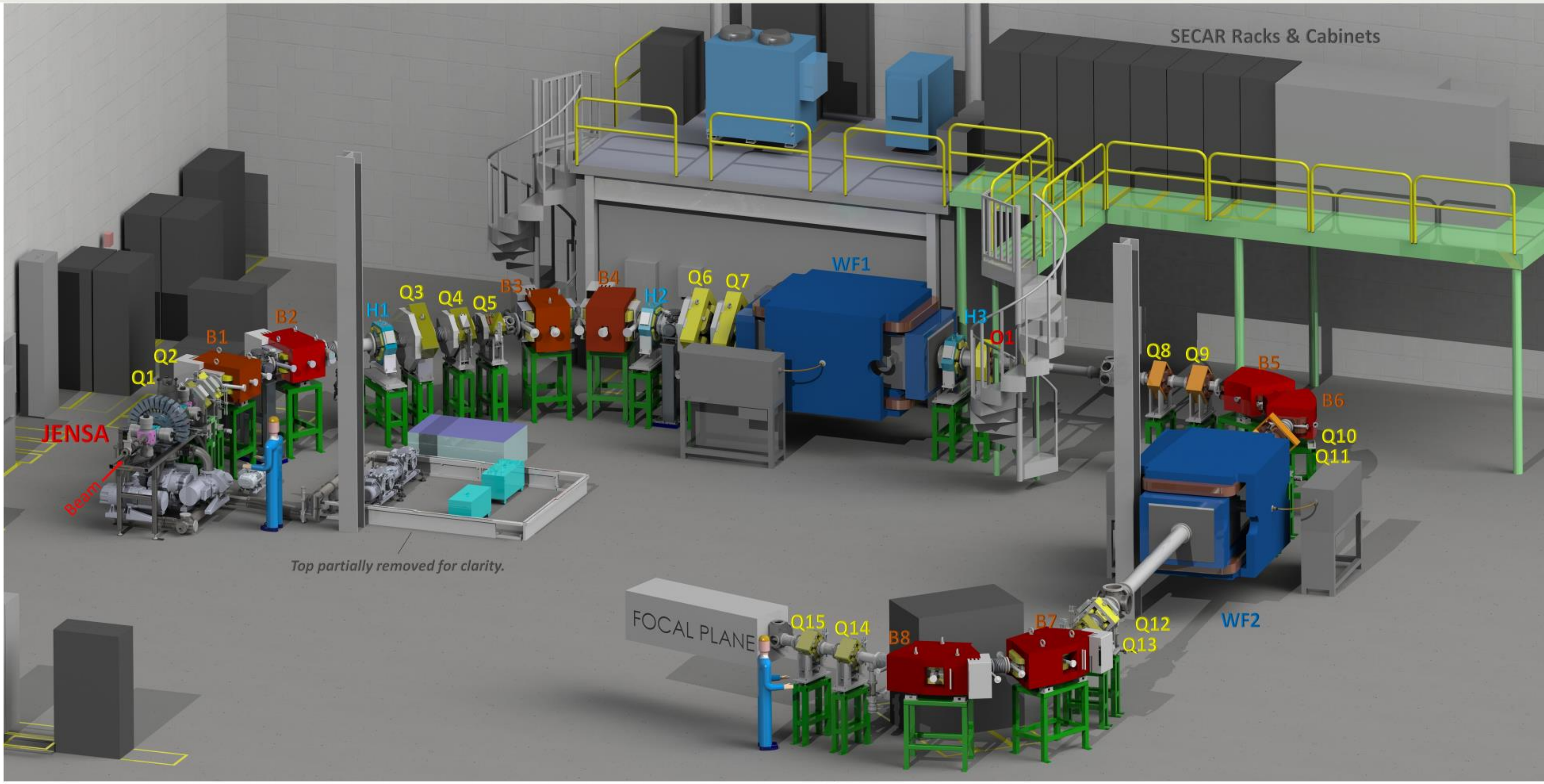

SECAR

Separator for Capture Reactions

Ion Optics Optimized

Charge B

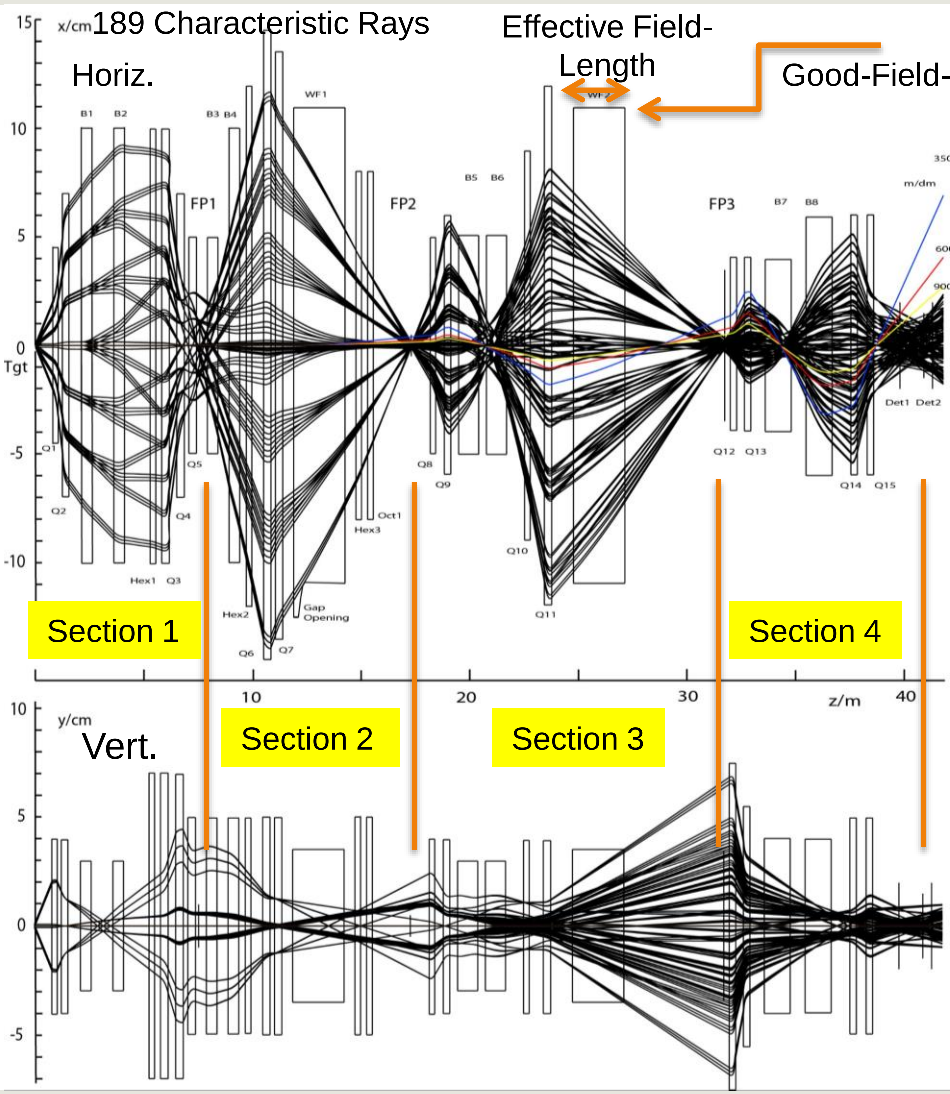

Section 1 Target to FP1

Charge state Selection

Dispersive focus

Section 2 FP1 to FP2

Mass Resolv. Power R_m = 747

Mass Resolution R_{HO} = 508

Achromatic focus

Section 3 FP2 to FP3

Mass Resolv. Power R_m =1283

Mass Resolution = 767

Disp. R_{16}=0, focus R_{12} = 0

Section 4 FP3 to Det1/Det2

Particle detection, HO correction

Cleanup section

Optimized up to 4^{th} order, using

4 Hexapoles, 1 Octupole

Dipole edges up to 4^{th} order

SECAR

End Lecture 3

Design Parameters of SECAR for the FRIB at MSU

Design parameters of the SECAR magnetic recoil separator.

Maximum rigidity Bρ	0.80 Tm
Minimum rigidity Bρ	0.14 Tm
Angle acceptance, vert., horiz.	$\pm$25 mrad
Energy acceptance	$\pm$ 3.1 %
Mass separation m/Δm	$\approx$ 800
Bending radius	125 cm

Direct measurement of astrophysically relevant (p,γ) reactions up to mass about 66 for the rp- process using radioactive beams of FRIB

SECAR with WF1

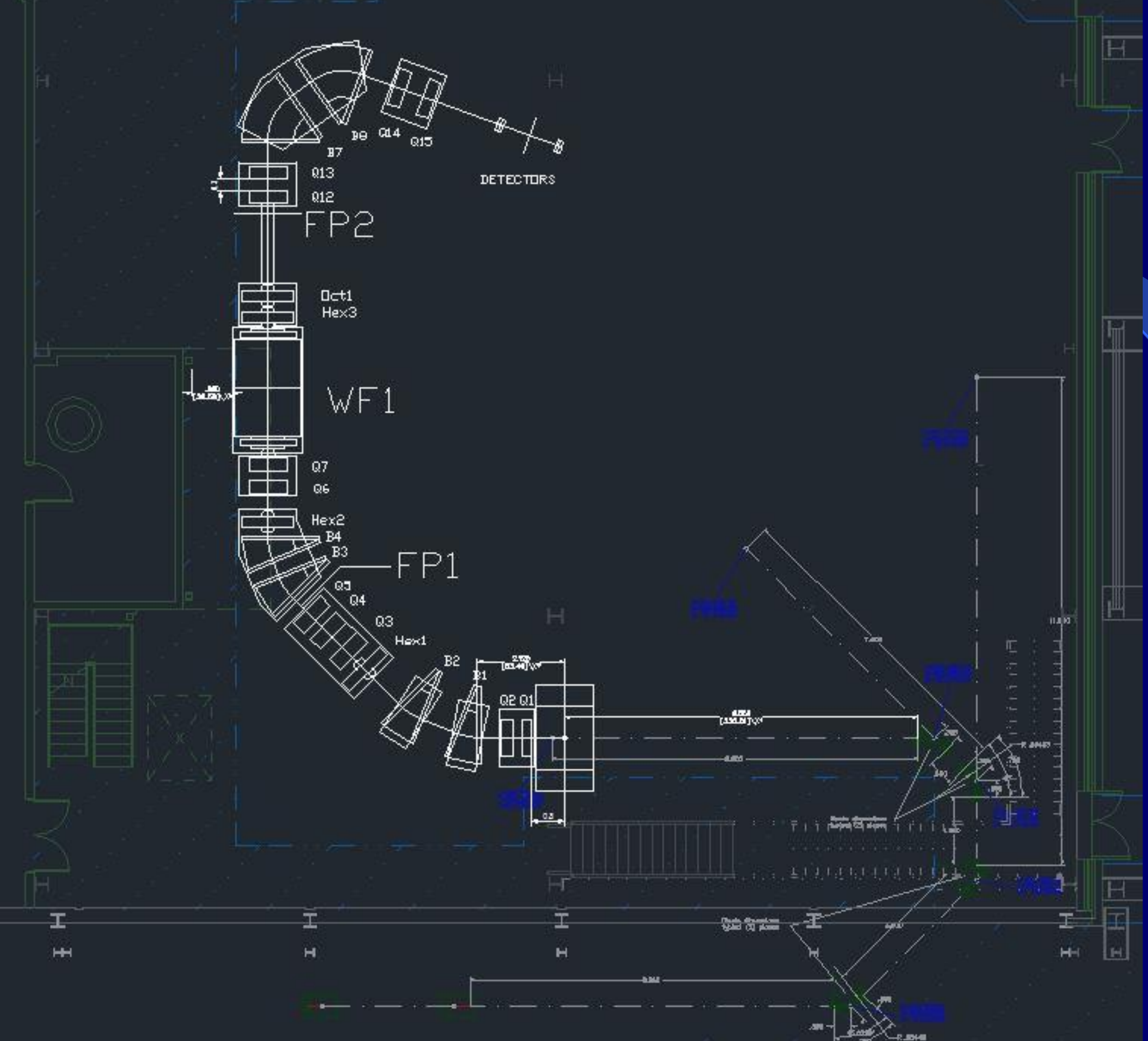

SECAR with WF1 and WF2

Radiative capture in inverse kinematics

Kinematics of produced ions

Recoil maximum aperture:

$$\theta_{\max} = \arctan\left(\frac{p_\gamma}{p^*}\right) = \arctan\left(\frac{E_\gamma / c}{\sqrt{2 m_b E_b}}\right)$$

$$p_r = p^* \pm p_\gamma$$

Nice BUT:

•Most of the beam does not interact

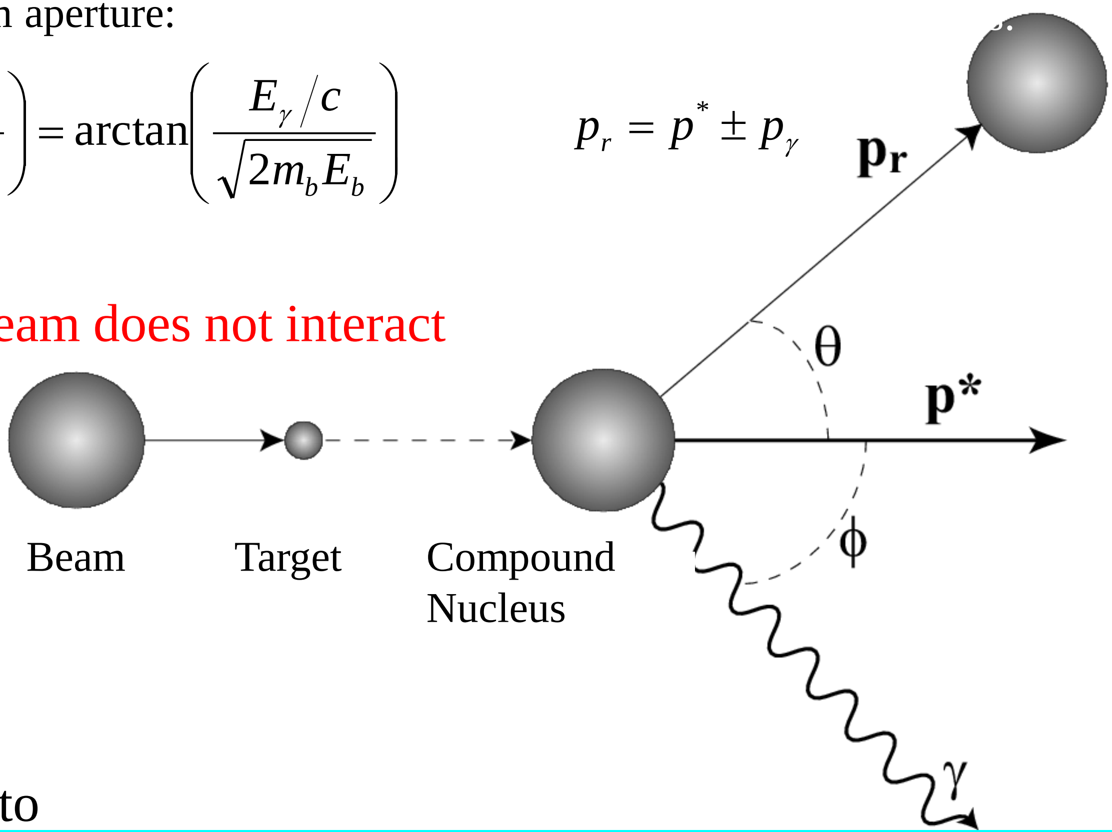

Need a system to

•Reject the beam

•Transport the recoils in a detector

This slide from: Manoël Couder

Beam and recoils have same momenta. No separation by B field alone, need E field.

Charge and Mass Separation

SECAR with cleanup and detector section

Simulation with m/dm=350
Achieved m/dm= 508

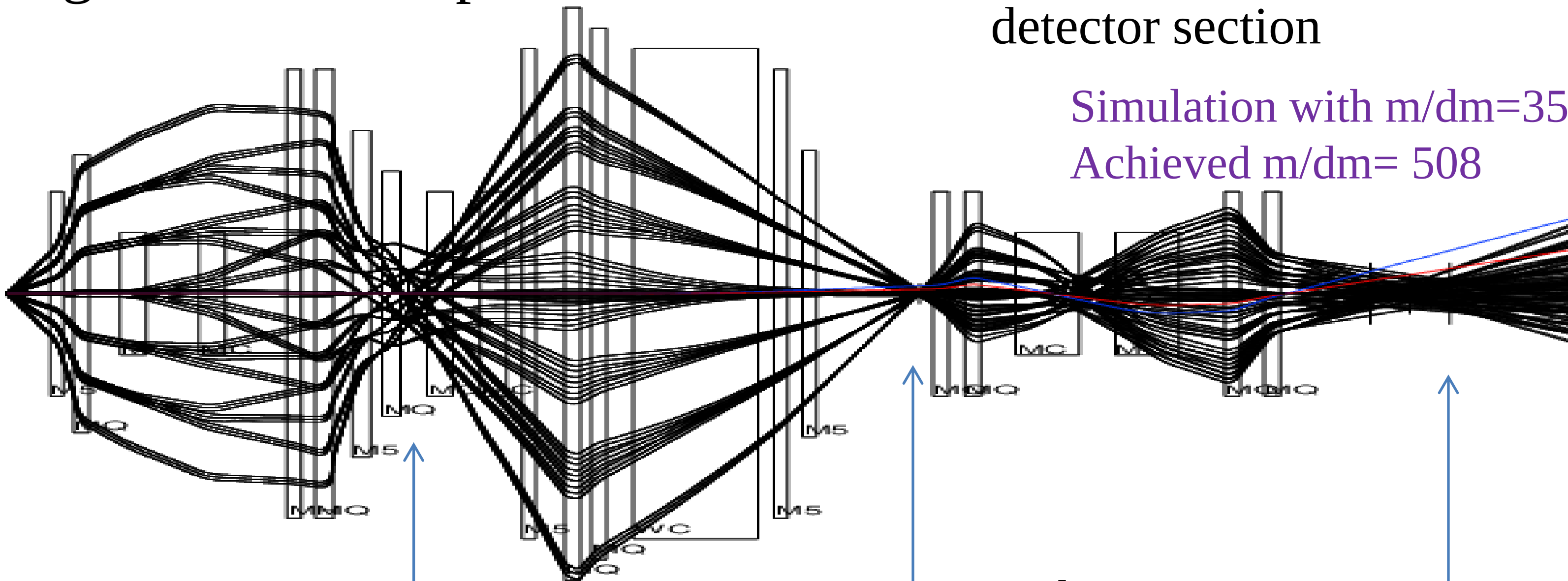

Charge state separation

Cleanup Section

RECOILS
m = 66

RECOILS
q=21

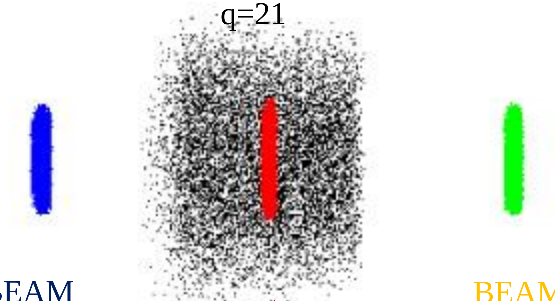

BEAM
q= 22

BEAM
q= 20

BEAM
q= 21

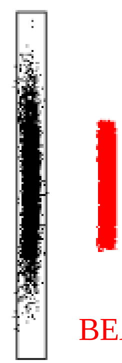

BEAM
m= 65

RECOILS
m = 66

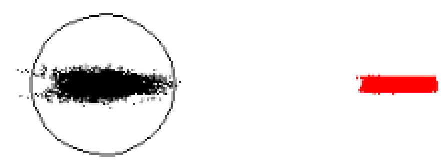

BEAM
m= 65

Monte Carlo Simulations with
10,000 rays by Manoel Couder

SECAR WF1

Charge state & Mass separation

Horizontal plane

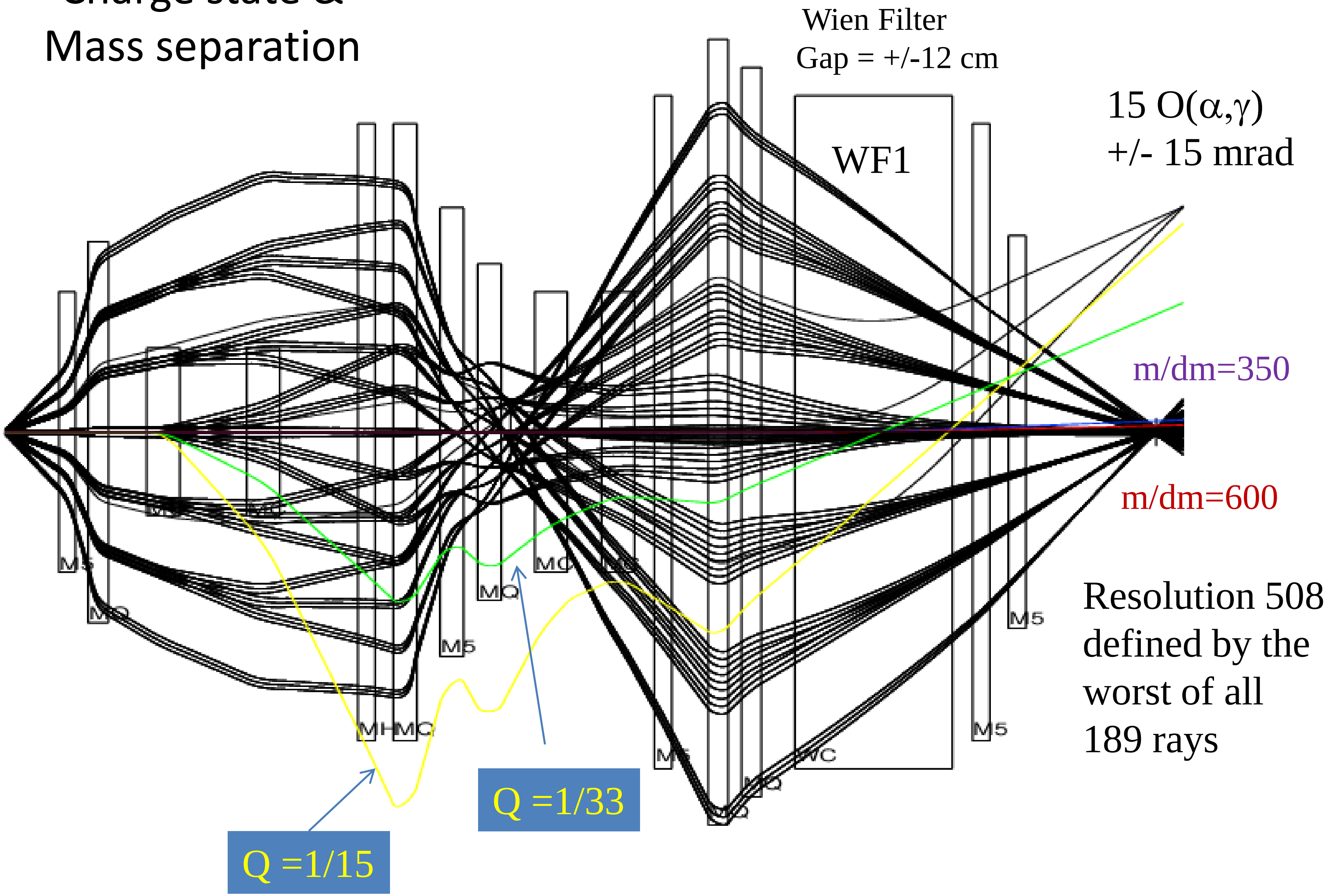

SECAR (2 WF) ion-optics with cleanup and detector section

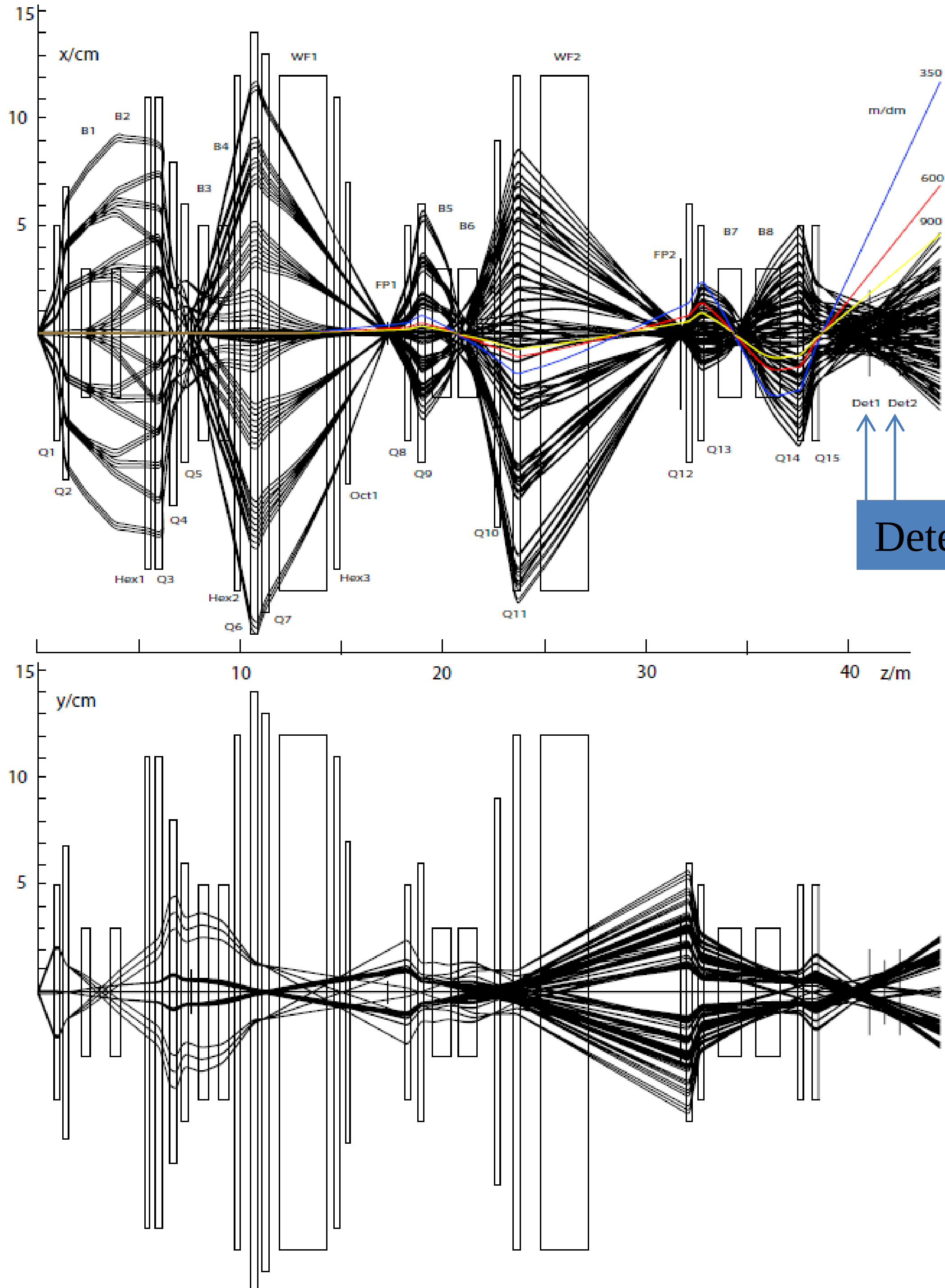

Corrected up to order 7

Resolution: m/dm=768 in FP2

Detectors, 3 cm dia, 150 cm distance

Used in optimization:

189 rays within ellipsoid A=B=25 mrad, dE/E=3.1%, and X=Y=+/- 0.75 mm

SECAR Wien filter

- Cross section in the center, Beam enters into the plane. The Good-Field-Region is indicated by dotted lines between the kidney shaped electrodeS

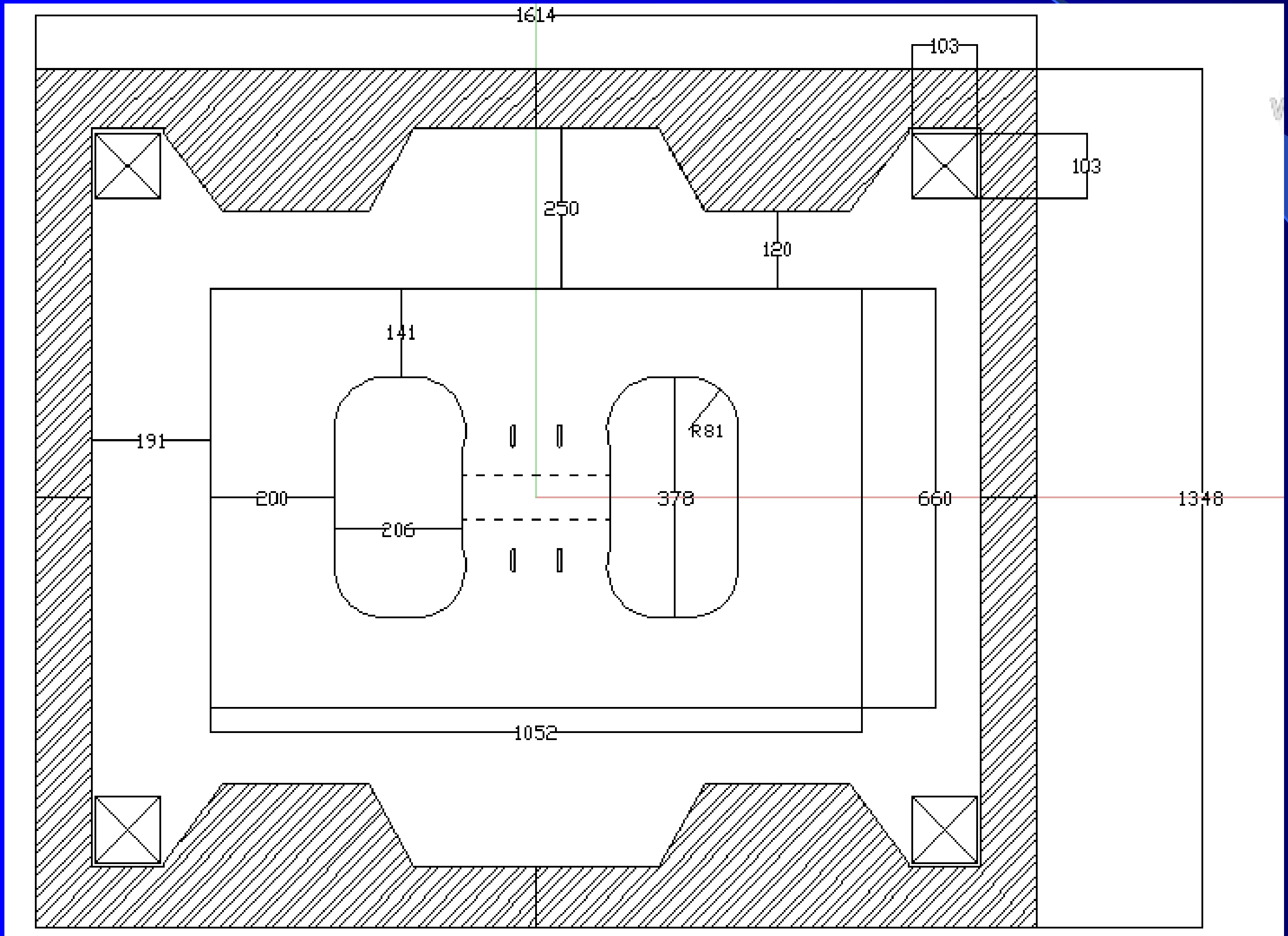

SECAR WF Parameters

SECAR Wien Filter			
Good-field region	horizontal	mm	220
	vertical	mm	40
Dipole magnet	Max. B field	T	0.12
	Effective field length	mm	2350
	Pole gap, vertical	mm	680
	Pole width	mm	1020
	B field, homogeneity		±0.002 in GFR
	Estimated power	kW	50
	Iron weight	kg	4000
	Weight of 2 coils	kg	1150
Electrostatic system	Max. E field	kV/mm	2.8
	Max. Voltage on electrodes	kV	± 300
	Max. Homigenizing electrode	kV	± 110
	Effective field length	mm	2350
	Electrode gap, horizontal	mm	220
	Electrode height, vertical	mm	378
	E field, homogeneity		±0.002 in GFR
	Electrode to grounded chamber	mm	141
	Max. E field in gap to wall	kV/mm	3.8
	2 Electrodes, Ti, non magn.	kg	approx. 1000
	Vacuum chamber, SS, non magn.	kg	approx. 1000